The abundant marine bacterium *Pelagibacter* simultaneously catabolizes dimethylsulfoniopropionate to the gases dimethyl sulfide and methanethiol

Jing Sun[1], Jonathan D. Todd[4], J. Cameron Thrash[5], Yanping Qian[2], Michael C. Qian[2], Ben Temperton[6], Jiazhen Guo[7], Emily K. Fowler[4], Joshua T. Aldrich[8], Carrie D. Nicora[8], Mary S. Lipton[8], Richard D. Smith[8], Patrick De Leenheer[3], Samuel H Payne[8], Andrew W. B. Johnston[4] Cleo L. Davie-Martin[1], Kimberly H. Halsey[1] and Stephen J. Giovannoni[1]*

[1]Department of Microbiology, [2]Department of Food Science, [3]Department of Mathematics, Oregon State University, Corvallis, Oregon 97331, USA; [4]School of Biological Sciences, University of East Anglia, Norwich Research Park, Norwich, NR4 7TJ, UK; [5]Department of Biological Sciences, Louisiana State University, Baton Rouge, LA, 70803, USA; [6]Plymouth Marine Laboratory, Prospect Pl, Plymouth, Devon PL1 3DH, UK. [7]Qingdao Aquarium, Qingdao, Shandong 266003, China. [8]Environmental Molecular Sciences Laboratory, Pacific Northwest National Laboratory, Richland, WA, 99352, USA.

Running title: DMSP metabolism in SAR11

* Corresponding Author

Department of Microbiology, Oregon State University, Corvallis, Oregon 97331

Phone: (541) 737-1835, Fax: (541) 737-0496

Email: steve.giovannoni@oregonstate.edu

Keywords DMSP, *Pelagibacter ubique*, SAR11(*Pelagibacterales*), DddK, DMSP lyase

Marine phytoplankton produce ~10^9 tons of dimethylsulfoniopropionate (DMSP) per year[1,2], an estimated 10% of which is catabolized by bacteria through the DMSP cleavage pathway to the climatically active gas dimethyl sulfide (DMS)[3,4]. SAR11 *Alphaproteobacteria* (order *Pelagibacterales*), the most abundant chemoorganotrophic bacteria in the oceans, have been shown to assimilate DMSP into biomass, thereby supplying this cell's unusual requirement for reduced sulfur[5,6]. Here we report that *Pelagibacter* HTCC1062 produces the gas methanethiol (MeSH) and that simultaneously a second DMSP catabolic pathway, mediated by a cupin-like DMSP lyase, DddK, shunts as much as 59% of DMSP uptake to DMS production. We propose a model in which the allocation of DMSP between these pathways is kinetically controlled to release increasing amounts of DMS as the supply of DMSP exceeds cellular sulfur demands for biosynthesis.

In an experiment designed to measure the stoichiometry of DMSP consumption, we observed that *Pelagibacterales* strain HTCC1062 produced MeSH, the gaseous end product of a catabolic pathway in which the first step involves DMSP demethylation. This was consistent with the presence in the genome of *dmdA*, which encodes DMSP demethylase[3,7]. However, we were surprised to observe that axenic cultures of this strain also produced large amounts of DMS (Fig. 1A). This observation indicated that, despite widespread attention to *Pelagibacterales* genomics and metagenomics, a *Pelagibacter* DMSP cleavage metabolic pathway leading to DMS formation had gone undetected. The amounts of DMS and MeSH increased linearly over 18 h of incubation in the presence of live cells, but DMS production by killed cell controls was either low or undetectable. Over 80% of the DMSP sulfur decrease could be accounted for, with 59% converted to DMS, 21% to MeSH, and ~1% for biosynthesis

(Table 1). These observations were confirmed by real time measurements of DMS and MeSH production by cultured cells, using a proton-transfer-reaction time-of-flight mass spectrometer (Fig. 2A).

The discovery that *Pelagibacter* expresses two DMSP degradation pathways simultaneously is particularly striking given its small genome size (1.28-1.46 Mb) and simplified metabolism[8]. Enzymes for the DMSP demethylation pathway (DmdABC) have been described in *Pelagibacter*, but not DmdD, which catalyzes the release of MeSH from methylthioacryloyl-CoA (MTA-CoA)[9]. Nor has a gene for any DMSP lyase, which catalyzes the alternate catabolic pathway leading to DMS production, been annotated or reported in *Pelagibacter*. Thus, the data shown in Fig. 1A confirm a complete demethylation pathway leading to MeSH production in *Pelagibacter*[3,7], and are the first evidence of a DMSP cleavage pathway in this organism.

Assimilation of DMSP sulfur into biomass is potentially a strong evolutionary driver for retention of DMSP metabolism in *Pelagibacterales*, which lack genes for assimilatory sulfate reduction[10]. To identify intermediates of DMSP metabolism that could support the demand for reduced sulfur for biosynthesis, HTCC1062 cultures were inoculated into artificial seawater media in the presence of MeSH, DMS, or methionine (Fig. 1B). Only MeSH and methionine supported growth above the negative control. This is the first data showing that free MeSH can serve as an S source for *Pelagibacterales* cells, and it is consistent with the observation that, under DMSP-replete conditions, more S is released as MeSH than is used for growth. The lower molar yield observed with MeSH, relative to methionine likely is a consequence of the

susceptibility of MeSH to spontaneous oxidation. DMS is apparently a metabolic waste product and cannot serve as a source of reduced sulfur in *Pelagibacterales*, in accord with the observations that DMS monooxygenase and DMS dehydrogenase are missing from *Pelagibacterales* genomes (Fig. S1).

The unexpected observation of DMS production by HTCC1062 cultures (Fig. 1A) suggested that a DMSP lyase gene had gone undetected in the genome[7,9]. Reviewing the genome annotation, we noticed that hypothetical gene SAR11_0394 was predicted to have a C-terminal cupin, a very widely distributed protein fold that resembles a small barrel[11]. Of the DMSP lyases identified to date, three (DddL, DddQ and DddW) have C-terminal cupin domains and are members of the cupin superfamily[12-14] (Fig. S2). We confirmed that the SAR11_0394 gene encoded a product with DMSP lyase activity, by cloning and expressing it in *E. coli* strain BL21; when grown in M9 medium containing 1 mM DMSP, the transformed *E. coli* strain converted ~15.4% of this substrate to corresponding molar amounts of DMS plus acrylate, as determined by GC and NMR respectively. Genes homologous to SAR11_0394 in two additional *Pelagibacterales* strains, HTCC9022 and HIMB5, were cloned and also confirmed to encode DMSP lyases (Table S1). The genes were named *dddK*. The DddK of HTCC1062 was purified and a V_{max} of 3.61 ± 0.27 μmol DMS min^{-1} mg protein $^{-1}$, and a K_m of 81.9 ± 17.2 mM, were determined (Fig. S3 and S4).

DMSP catabolism also benefits cells by providing a source of organic carbon that can be oxidized for energy production or assimilated into biomass[15]. The data suggest that when cells are supplied with an excess of DMSP, 59% of DMSP oxidation likely is supporting carbon

metabolism (Fig. 1A, Table 1). DMSP lyase enzymes are distributed among multiple protein families, but all lead to the production of DMS and either acrylate (DddL,P,Q,W,Y) or 3-hydroxypropionate (3-HP; DddD)[9]. The HTCC1062 genome encodes annotated genes for all steps in the degradation of acrylate to propionyl-CoA or acetyl-CoA (Fig. 3). To test the capacity of strain HTCC1062 to assimilate acrylate, propionate or 3-HP, we relied on the unusual requirement of *Pelagibacter* strains for growth substrates that can be metabolized to pyruvate, which these cells require for alanine synthesis[16]. As predicted, acrylate and propionate each could substitute for pyruvate in defined media. Enhancement of growth by 3-HP was slight, but statistically significant (Student's t test, n=3, $P<0.05$), (Fig. 1C).

Comparisons of *Pelagibacterales* genomes across the Group Ia subclade revealed that *dddK* homologues were found in eight of twelve *Pelagibacterales* Ia genomes (Fig. S5). In addition to *dddK*, strain HIMB5 has a homolog of *dddQ*, also a member of the cupin superfamily[13]. As predicted, *E. coli* transformants containing cloned HIMB5_00000220 (*dddQ*) displayed DMSP lyase activity (K_m was 56 mM, V_{max} was 0.78 μmol min^{-1} mg $protein^{-1}$). Strain HTCC7211 and the more distantly related subclade V strain HIMB59 lacked *dddK* homologues, but encoded gene products (respectively PB7211_1082 and HIMB59_00005110) that are ~30% identical to DddP, a DMSP lyase in the M24 family of metallo-peptidases[17,18]. However, *E. coli* transformants containing cloned PB7211_1082 (*dddP*-like) showed very low DMSP lyase activity (0.5 ± 0.1 nmol min^{-1} mg^{-1}), and therefore this protein may not be bona fide DMSP lyases.

We compared the abundance of the *Pelagibacterales* genes for DMSP cleavage with those

for demethylation (*dmdABC*) in the Global Ocean Survey (GOS) metagenomic dataset (Fig. S6). The DMSP lyases *dddK* and *dddQ*, and *dddP*, the putative lyase with low activity, were much less abundant than *dmdABC* or the single-copy marker *recA*. This supports the interpretation that either the cleavage pathway is less important than the demethylation pathway, or undiscovered DMSP lyase analogs are present in other *Pelagibacterales* strains. Interestingly, *Pelagibacterales* genes for metabolism of acrylate are more abundant than DMSP lyases, and similar in abundance to demethylation genes and *recA*, which supports either the interpretation that DMSP lyases are underestimated because of their diversity, or that *Pelagibacter* cells lacking DMSP lyase use acrylate from other sources, perhaps dissolved acrylate.

Most of the *Pelagibacterales* strains with DddK genes belong to the temperate surface ocean ecotypes (Ia.1) [19], whereas most of the strains that possess DddP are subtropical ocean surface ecotypes (Ia.3) (Fig. S5). This may indicate that the lyase system is more common in *Pelagibacterales* strains, such as HTCC1062, that originate from higher productivity ocean regions, a distribution that is consistent with its inferred role as an auxiliary system that metabolizes excess DMSP. However the presence of an alternate gene, DddP, that has weak DMSP lyase activity in most SAR11 Ia.3 strains, suggests that further investigations of the phenotypes of live strains will be needed before the distribution of DMSP metabolism across the clade is fully understood.

Metabolic reconstruction with eight *Pelagibacterales* genomes revealed that, consistent with the observation of MeSH production in HTCC1062, this and other examined *Pelagibacterales* strains, except those in the distantly related subclade IIIa, contain homologs

of the *dmdABC* genes found in *Ruegeria pomeroyi*[20] (Fig. S1). Also reported in nearly all *Pelagibacterales* are genes encoding methyl group oxidation pathways (Fig. S1), which produce energy from DMSP demethylation and are essential to the demethylation pathway because they perform the function of regenerating the methyl-group-accepting cofactor tetrahydrofolate (THF)[15,20]. *Pelagibacterales* strains also contain homologs of cystathionine-gamma-synthetase (cys-γ-synth), predicted to catalyze the conversion of MeSH to methionine[21], and thus necessary for growth using MeSH as a sole sulfur source. However, none of these examined *Pelagibacterales* strains had homologs of *dmdD* (methylthioacryloyl-CoA hydratase), which converts MTA-CoA to MeSH. The absence of this gene from *Pelagibacterales* is also reflected in its low abundance in ocean metagenomic databases[9]. As in HTCC1062, *dmdD* is not required for complete demethylation of DMSP to MeSH in *Ruegeria lacuscaerulensis*[7], suggesting that an un-described analogous enzyme fills this pathway gap.

One of the unexpected findings reported above is that both the cleavage and demethylation pathways operate simultaneously. We investigated transcription changes using Affymetrix microarrays and observed no significant changes in the expression of DMSP catabolic pathway genes between HTCC1062 cells grown in the presence and absence of DMSP (see Supplementary Note II). Since no changes in transcription were observed, we used isobaric tags for relative and absolute quantitation (iTRAQ) to compare the proteomes of HTCC1062 cultures grown in the presence and absence of DMSP, confirming that proteins for both pathways of DMSP catabolism are expressed constitutively (Fig. S7, Table S2). Further support for this conclusion came from real-time measurements of DMS and MeSH production by cells, which showed that DMS and MeSH were immediately released by cells that had been grown

in the absence of DMSP when DMSP was added (Fig. 2A).

We propose that constitutive, simultaneous expression of the cleavage and demethylation pathways in *Pelagibacter* is an adaptation that provides these cells with a kinetically regulated system that favors the pathway to DMS formation when intracellular DMSP concentrations are high. We modeled this process (Fig. S8) using the measured properties of cloned enzymes and intracellular DMSP concentration (Fig. 2B). In *Pelagibacter*, DMSP active transport is thought to be mediated by the ABC transporter (OpuAC), which was the sixth most highly detected *Pelagibacterales* protein in a previous study of the Sargasso Sea metaproteome[22]. The properties of ABC transport functions are consistent with the model in that they predict that cells can achieve high intracellular DMSP concentrations from naturally measured DMSP abundances (Table S3), provided that DMSP remains within the range of transporter affinity for a period of hours (see Supplementary Note V). The K_m we measured for DddK, 81.9 ± 17.2 mM (Fig. S4), is high relative to the K_m of DmdA (13.2 ± 2.0 mM)[23]. Intracellular DMSP concentrations increased following DMSP addition, reaching a maximum of 180 mM after four hours (Fig. 2B). When DMSP flux into cells is low, the model predicts that most is channeled to MeSH production, producing energy via oxidation of the products CH_3-THF and acetaldehyde, sulfur for biosynthesis, and MeSH losses caused by oxidation and diffusion (Fig. 1A). As intracellular DMSP concentrations rise, the model predicts that DMSP cleavage to DMS increases (Fig. S8). There is a precedent for simple, kinetically driven switches controlling the flow of vital metabolites in HTCC1062, where intracellular glycine concentrations control the flow of carbon from exometabolites, such as glycolic acid, via glycine-mediated riboswitches[16,24]. Kinetic regulation of metabolic processes is well known,

but here we see evidence that it plays an unexpected role in large-scale biogeochemical processes mediated by metabolically streamlined cells.

The model presented in Fig. S8 captures the observations we report, and provides an explanation for why cells might simultaneously express two pathways that compete for a single substrate. Although the model in Fig. S8 is based on in vitro enzyme kinetics, which can deviate from the kinetic properties of enzymes in the intracellular environment, the model successfully approximated the behavior of whole cells (Fig. 2A). However, a number of aspects of this model will need to be tested and refined before it can be validly implemented for geochemical predictions. In particular, we observed cells accumulating DMSP to high intracellular concentrations over a period of a few hours when supplied with excess DMSP. It remains to be determined how frequently such sustained supplies of DMSP occur in nature.

Recognition that the relative expression of the demethylation and cleavage pathways by bacteria in nature controls the fate of DMSP sulfur led to a concept that is referred to as the 'bacterial switch' in discussions of DMSP biogeochemistry[2]. In principle, the 'bacterial switch' could involve different bacterial taxa, each potentially having a different organization of DMSP metabolic pathways. Although the bacterial switch is largely hypothetical[4,25,26], insight has emerged from studies of cells in culture. Like *Pelagibacter*, the marine bacterium *R. pomeroyi* strain DSS-3 has both the DMSP demethylation and cleavage pathways, which are transcriptionally regulated, although the changes in expression that were reported were not very large[18,27]. Further work is needed to determine whether kinetic switching plays a role in the *R. pomeroyi* response to DMSP. Recent field observations indicate that *Roseobacter* species HTCC2255 regulates transcriptional expression of both the lyase and demethylase pathways

for DMSP catabolism in response to changing environmental conditions[28]. The findings we report here provide important details about the mechanisms of the bacterial switch that will be vital to the design of future research and to modeling transformations of DMSP in ocean ecosystems[29,30]. Many factors, including DMSP leakage from phytoplankton, the action of free (dissolved) DMSP-lyases, and the activity of many different microbial taxa, contribute to natural fluxes of DMSP and its volatile derivatives[28,29]. The findings we present here describe an unexpected and simple mechanism that is likely an important part of this complex process.

Methods Summary

Measurements of DMSP and its metabolic products:

HTCC1062 was grown in autoclaved, filtered artificial seawater (ASW)[16] amended with 1 mM NH_4Cl, 100 μM KH_2PO_4, 1 μM $FeCl_3$, 100 μM pyruvate, 50 μM glycine, 1 μM DMSP, and excess vitamins[16]. Cultures were harvested by centrifugation, washed once, and resuspended in ASW. Cells (final concentration was ~1.5×10^6 cells mL^{-1}) were distributed into 20 mL sealed vials (10 mL /vial). 1 μM DMSP was injected into vials and were incubated in the dark at 16 °C. Biological activities were stopped by addition of 0.1 M sodium azide (100 μL/vial) at 0 min, 20 min, 1 h, 3 h, 9 h and 18 h. Duplicate samples were refrigerated before chemical analysis.

DMS and MeSH were analyzed using the solid-phase microextraction-gas chromatography-pulsed flame-photometric detection (SPME-GC-PFPD) method[31,32]. DMSP was quantified by measuring released DMS after hydrolysis in NaOH (0.1 M final concentration), at room temperature for 12 h.

DMS & MeSH utilization in HTCC1062

HTCC1062 was cultured in 40 mL clear sealed vials with autoclaved, filtered ASW amended with 1 mM NH_4Cl, 100 μM KH_2PO_4, 1 μM $FeCl_3$, 100 μM pyruvate, 50 μM glycine, excess vitamins[16] and 100 nM DMSP, methionine, DMS or MeSH. Each vial contained a 10 mL aliquot, which was incubated on a shaker at 16℃. Cell densities were monitored with a Guava flow cytometer[33].

C3 compounds utilization in HTCC1062

Cells were grown in autoclaved, filtered ASW amended with 100 μM NH_4Cl, 10 μM KH_2PO_4, 100 nM $FeCl_3$, 50 μM glycine, 50 μM methionine, and excess vitamins[16]. Each compound (3-HP, acrylate or propionate) was tested at a concentration of 10 μM. The positive control was amended with 10 μM pyruvate. The negative control contained no pyruvate.

Real-time measurements of DMS and MeSH by PTR-TOF/MS

HTCC1062 was grown in autoclaved, filtered ASW amended with 1 mM NH_4Cl, 100 μM KH_2PO_4, 1 μM $FeCl_3$, 100 μM pyruvate, 25 μM glycine, 25 μM methionine, and excess vitamins[16]. Cultures were harvested by centrifugation, washed once, and re-suspended in ASW. Cells ($3\sim5\times10^6$ cells mL^{-1} final concentration) were distributed into 100 mL of ASW and placed in a 200 mL polycarbonate dynamic stripping chamber. 1 μM DMSP was spiked into the chamber and the suspensions were incubated at 16 °C under a continuous flow of fine air bubbles. A proton-transfer-reaction time-of-flight mass spectrometer (PTR-TOF 1000, IONICON Analytik, Innsbruck, Austria) was used to quantify the production of MeSH and DMS from HTCC1062 cultures. The fundamentals of PTR-MS are described elsewhere[34].

Primary ions (protonated water, H_3O^+) were produced from pure water vapor in the hollow cathode ion source at a flow rate of 5 sccm, from which they entered the drift tube. The sample air stream produced from the dynamic stripping chamber was introduced to the drift tube via a separate orifice, where proton transfer reactions occurred between H_3O^+ and volatile organic compounds (VOCs) that had proton affinities greater than that of water (691 kJ mol^{-1}):

$$VOC + H_3O^+ \rightarrow VOC{\cdot}H^+ + H_2O$$

Within the drift tube, the pressure, temperature, and voltage conditions were kept constant at 2.0 mbar, 80 °C, and 600 V, respectively, which equated to a field strength (*E/N*) of 153 Td (where Td = 10^{-17} cm^2 V $molecule^{-1}$). One advantage of PTR-MS is that reactions occurring in the drift tube are non-dissociative and thus, compounds are usually not fragmented during ionization and exhibit a protonated mass of M+1. Thus, for DMS and MeSH, we monitored m/z 63 and 49, respectively. Although interference at these masses is likely to be low, we cannot rule out the possibility that more than one compound was contributing to the signal. Mass spectra were recorded up to 250 amu at 10 s integration intervals. Quantification of gas-phase DMS and MeSH concentrations was achieved using the relative transmission (kinetic) approach and additionally accounted for the influence of the hydrated water cluster at m/z 37 (due to the high sample humidity introduced by bubbling air through seawater). For MeSH, a default collision rate constant of $2.00x10^{-9}$ cm^{-2} was assumed, whereas a literature value of $2.53x10^{-9}$ cm^{-2} was used for DMS[35].

Intracellular DMSP concentration

HTCC1062 was grown in the same condition mentioned above (See methods of Real-

time measurements of DMS and MeSH by PTR-TOF/MS). Cultures were harvested by centrifugation, washed once and resuspended in ASW. Cells (~4×10^6 cells mL^{-1} final concentration) were distributed into five 200 mL chambers (100 mL/chamber) and treated using the same air bubbling method as described for the dynamic stripping chambers above. 1 µM DMSP was spiked into the chambers, which were subsequently incubated at 16 °C. Duplicate negative (killed cells) controls were performed by addition of 0.1 M sodium azide (100 µL/vial). 10 mL cultures were filtered through 0.1 µm PTFE membranes at 10min, 1.5h, 4h. 7h, 10h and 13h. The cells on the membranes were washed once with ASW, then transferred into 20 mL sealed vials, and finally resuspended in 10 mL ASW. DMSP was quantified by measuring DMS release after hydrolysis in NaOH (0.1 M final concentration), at room temperature for 12 h. DMS was analyzed using the SPME-GC-PFPD method.

References

1 Curson, A. R. J., Todd, J. D., Sullivan, M. J. & Johnston, A. W. B. Catabolism of dimethylsulphoniopropionate: microorganisms, enzymes and genes. *Nature Reviews Microbiology*, 1-11, doi:10.1038/nrmicro2653 (2011).

2 Simó, R. Production of atmospheric sulfur by oceanic plankton: biogeochemical, ecological and evolutionary links. *Trends in Ecology & Evolution* **16**, 287-294 (2001).

3 Reisch, C. R., Moran, M. A. & Whitman, W. B. Bacterial catabolism of dimethylsulfoniopropionate (DMSP). *Frontiers in Microbiology* **2**, 172, doi:10.3389/fmicb.2011.00172 (2011).

4 Kiene, R. P., Linn, L. J. & Bruton, J. A. New and important roles for DMSP in marine microbial communities. *Journal of Sea Research* **43**, 209-224, doi:10.1016/S1385-1101(00)00023-X (2000).

5 Malmstrom, R. R., Kiene, R. P., Cottrell, M. T. & Kirchman, D. L. Contribution of SAR11 bacteria to dissolved dimethylsulfoniopropionate and amino acid uptake in the North Atlantic ocean. *Applied and Environmental Microbiology* **70**, 4129-4135, doi:10.1128/AEM.70.7.4129-4135.2004 (2004).

6 Vila-Costa, M., Pinhassi, J., Alonso, C., Pernthaler, J. & Simó, R. An annual cycle of dimethylsulfoniopropionate-sulfur and leucine assimilating bacterioplankton in the coastal NW Mediterranean. *Environmental Microbiology* **9**, 2451-2463, doi:10.1111/j.1462-2920.2007.01363.x (2007).

7 Reisch, C. R. *et al.* Novel pathway for assimilation of dimethylsulphoniopropionate widespread in marine bacteria. *Nature* **473**, 208-211, doi:10.1038/nature10078 (2011).

8 Giovannoni, S. J., Cameron Thrash, J. & Temperton, B. Implications of streamlining theory for microbial ecology. *ISME J*, doi:10.1038/ismej.2014.60 (2014).

9 Moran, M. A., Reisch, C. R., Kiene, R. P. & Whitman, W. B. Genomic insights into bacterial DMSP transformations. *Annual Review of Marine Science* **4**, 523-542, doi:10.1146/annurev-marine-120710-100827 (2012).

10 Tripp, H. J. *et al.* SAR11 marine bacteria require exogenous reduced sulphur for growth. *Nature* **452**, 741-744, doi:10.1038/nature06776 (2008).

11 Dunwell, J. M., Purvis, A. & Khuri, S. Cupins: the most functionally diverse protein superfamily? *Phytochemistry* **65**, 7-17, doi:10.1016/j.phytochem.2003.08.016 (2004).

12 Curson, A. R. J., Rogers, R., Todd, J. D., Brearley, C. A. & Johnston, A. W. B. Molecular genetic analysis of a dimethylsulfoniopropionate lyase that liberates the climate-changing gas dimethylsulfide in several marine α-proteobacteria and *Rhodobacter sphaeroides*. *Environmental Microbiology* **10**, 757-767, doi:10.1111/j.1462-2920.2007.01499.x (2008).

13 Todd, J. D. *et al.* DddQ, a novel, cupin-containing, dimethylsulfoniopropionate lyase in marine roseobacters and in uncultured marine bacteria. *Environmental Microbiology* **13**, 427-438, doi:10.1111/j.1462-2920.2010.02348.x (2011).

14 Todd, J. D., Kirkwood, M., Newton-Payne, S. & Johnston, A. W. DddW, a third DMSP lyase in a model Roseobacter marine bacterium, *Ruegeria pomeroyi* DSS-3. *ISME J* **6**, 223-226, doi:10.1038/ismej.2011.79 (2012).

15 Sun, J. *et al.* One carbon metabolism in SAR11 pelagic marine bacteria. *PloS One* **6**, e23973, doi:10.1371/journal.pone.0023973 (2011).

16 Carini, P., Steindler, L., Beszteri, S. & Giovannoni, S. J. Nutrient requirements for growth of the SAR11 isolate '*Candidatus* Pelagibacter ubique' HTCC1062 on a defined medium. *ISME J* **7**, 592-602, doi:doi:10.1038/ismej.2012.122 (2013).

17 Kirkwood, M., Le Brun, N. E., Todd, J. D. & Johnston, A. W. B. The *dddP* gene of *Roseovarius nubinhibens* encodes a novel lyase that cleaves dimethylsulfoniopropionate into acrylate plus dimethyl sulfide. *Microbiology* **156**, 1900-1906, doi:10.1099/mic.0.038927-0 (2010).

18 Todd, J. D., Curson, A. R. J., Sullivan, M. J., Kirkwood, M. & Johnston, A. W. B. The *Ruegeria pomeroyi acuI* gene has a role in DMSP catabolism and resembles *yhdH* of *E.*

coli and other bacteria in conferring resistance to acrylate. *PloS One* **7**, e35947, doi:10.1371/journal.pone.0035947 (2012).

19 Kevin, L. V. *et al.* High-resolution SAR11 ecotype dynamics at the Bermuda Atlantic Time-series Study site by phylogenetic placement of pyrosequences. *The ISME Journal* **7**, 1322-1332, doi:10.1038/ismej.2013.32 (2013).

20 Grote, J. *et al.* Streamlining and core genome conservation among highly divergent members of the SAR11 clade. *mBio* **3**, doi:10.1128/mBio.00252-12 (2012).

21 Kiene, R. P., Linn, L. J., González, J., Moran, M. A. & Bruton, J. A. Dimethylsulfoniopropionate and methanethiol are important precursors of methionine and protein-sulfur in marine bacterioplankton. *Applied and Environmental Microbiology* **65**, 4549-4558 (1999).

22 Sowell, S. M. *et al.* Transport functions dominate the SAR11 metaproteome at low-nutrient extremes in the Sargasso Sea. *ISME J* **3**, 93-105, doi:10.1038/ismej.2008.83 (2009).

23 Reisch, C. R., Moran, M. A. & Whitman, W. B. Dimethylsulfoniopropionate-dependent demethylase (DmdA) from *Pelagibacter ubique* and *Silicibacter pomeroyi*. *Journal of Bacteriology* **190**, 8018-8024, doi:10.1128/JB.00770-08 (2008).

24 Tripp, H. J. *et al.* Unique glycine-activated riboswitch linked to glycine-serine auxotrophy in SAR11. *Environmental Microbiology* **11**, 230-238, doi:10.1111/j.1462-2920.2008.01758.x (2009).

25 Gonzalez, J. M., Kiene, R. P. & Moran, M. A. Transformation of sulfur compounds by an abundant lineage of marine bacteria in the α-Subclass of the class Proteobacteria.

Applied and Environmental Microbiology **65**, 3810-3819 (1999).

26 Gonzalez, J. M. *et al. Silicibacter pomeroyi* sp. nov. and *Roseovarius nubinhibens* sp. nov., dimethylsulfoniopropionate-demethylating bacteria from marine environments. *International Journal Systematic Evolutionary Microbiology* **53**, 1261-1269 (2003).

27 Burgmann, H. *et al.* Transcriptional response of *Silicibacter pomeroyi* DSS-3 to dimethylsulfoniopropionate (DMSP). *Environmental microbiology* **9**, 2742-2755, doi:10.1111/j.1462-2920.2007.01386.x (2007).

28 Varaljay, V. A. *et al.* Single-taxon field measurements of bacterial gene regulation controlling DMSP fate. *ISME J* **9**, 1677-1686, doi:10.1038/ismej.2015.23 (2015).

29 Vallina, S. M. *et al.* A dynamic model of oceanic sulfur (DMOS) applied to the Sargasso Sea: Simulating the dimethylsulfide (DMS) summer paradox. *Journal of Geophysical Research: Biogeosciences* **113**, G01009, doi:10.1029/2007jg000415 (2008).

30 Polimene, L., Archer, S., Butenschön, M. & Allen, J. I. A mechanistic explanation of the Sargasso Sea DMS “summer paradox”. *Biogeochemistry* **110**, 243-255, doi:10.1007/s10533-011-9674-z (2012).

31 Fang, Y. & Qian, M. C. Sensitive quantification of sulfur compounds in wine by headspace solid-phase microextraction technique. *Journal of Chromatography, A* **1080**, 177-185 (2005).

32 Vazquez-Landaverde, P. A., Torres, J. A. & Qian, M. C. Quantification of trace volatile sulfur compounds in milk by solid-phase microextraction and gas chromatography-pulsed flame photometric detection. *Journal of Dairy Science* **89**, 2919-2927 (2006).

33 Tripp, H. J. Counting marine microbes with Guava Easy-Cyte 96 well plate reading flow

cytometer. *Protocol Exchange*, doi:doi:10.1038/nprot.2008.29 (2008).

34 Lindinger, W., Hansel, A. & Jordan, A. On-line monitoring of volatile organic compounds at pptv levels by means of proton-transfer-reaction mass spectrometry (PTR-MS) medical applications, food control and environmental research. *International Journal of Mass Spectrometry and Ion Processes* **173**, 191-241, doi:http://dx.doi.org/10.1016/S0168-1176(97)00281-4 (1998).

35 Zhao, J. & Zhang, R. Proton transfer reaction rate constants between hydronium ion (H3O+) and volatile organic compounds. *Atmospheric Environment* **38**, 2177-2185, doi:http://dx.doi.org/10.1016/j.atmosenv.2004.01.019 (2004).

Acknowledgments

The authors would like to thank Dr. John W. H. Dacey for kindly providing DMSP, and Dr. Emmanuel Boss for help modeling transport kinetics. We are grateful to Dr. John W. H. Dacey and Dr. Samuel Bennett for the advice on the methods of DMSP measurements, and Dr. Nick Le Brun for helpful suggestions on the properties of the cupin lyases and kinetics analysis. J. S. thanks China Scholarships Council (CSC) for financial support. Major support was provided by a grant from the Marine Microbiology Initiative of the Gordon and Betty Moore

Foundation grant GBMF607.01 to S. J. G.. Proteomics measurements were supported by the US Department of Energy's (DOE) Office of Biological and Environmental Research (OBER) Pan-omics program at Pacific Northwest National Laboratory (PNNL), and performed in the Environmental Molecular Sciences Laboratory, a DOE OBER national scientific user facility on the PNNL campus. A. W. B. J. and J. D. T. were supported by grant NE/H008586/1 from the UK Natural Environment Research Council and E. K. F. by a studentship from the Tyndall Centre at UEA. Funds for the PTR-TOF were provided by NASA through grant NNX15AE70G to K. H. H. and S. J. G and by a grant to K. H. H. by the OSU Research Office.

Author Contributions

J. S. and S. J. G conceived and designed the experiments. J. S., Y. Q., M. C. Q measured DMSP products and intracellular DMSP concentration. J. S. and J. G performed the physiological growth experiments of HTCC1062. J. S. and J. C. T. analyzed and proposed DMSP metabolic pathways. J. D. T., E. K. F., and A. W. B. J. designed and implemented the clone, expression and characterization of DddK. B. T. performed metagenomics analyses. B. T., J. T. A., C. D. N., M. S. L., R. D. S., and S. H. P. performed iTRAQ and data analyses. P. D. and S. J. G. proposed the model. C. L. D. and K. H. H measured real-time DMS/MeSH production by PTR-TOF/MS. S. J. G contributed reagents/materials/analysis tools.

Competing Financial Interests

The authors declare no competing financial interests.

Figure Legends

Figure 1. DMSP metabolism in HTCC1062. **A)** Accumulated sulfur gas in headspaces as a function of time. DMS or MeSH production from DMSP (Left Y axis) and DMSP decline (Right Y axis) in HTCC1062 culture. Results are the average of duplicate samples and error bars show the range of the duplicates. When the error bars are invisible, they are smaller than the size of the symbols. Killed cell controls were performed in single vials and the last data point for the killed cell (DMSP) was absent. No MeSH was detected in killed-cell controls. The Pearson's correlation P-value for the DMSP regression is 0.007, with correlation of -0.726. **B)** Utilization of MeSH and DMS by HTCC1062. Cultures were incubated in ASW amended with methionine (positive control), MeSH, or DMS. A culture without any sulfur source was treated as the negative control. Each point represents a single vial, and the experiments were repeated three times, with similar results. **C)** Utilization of C3 compounds. Cultures were incubated in ASW amended with 10 μM pyruvate (positive control), 3-HP, acrylate and propionate. The culture without pyruvate was treated as negative control. Points are the average density of triplicate cultures and error bars show the standard deviation (n=3). Student's t test was used to determine the significant difference between samples for each time point.

Figure 2. A) Real-time gas-phase MeSH and DMS production measurements by PTR-TOF/MS. HTCC1062 cell suspensions that were not previously exposed to DMSP were incubated in ASW and subjected to a flow of fine bubbles. 1 μM DMSP was added at T=0 to cells that had been grown in the absence of DMSP. Measurements are presented in relative concentration units and were normalized to the gas-phase concentrations of MeSH and DMS (m/z 49 and 63, respectively) at T=0. This experiment was repeated three times, with similar results, but variation that we attribute to differences between batch cultures (see also Fig. S9). **B)**

Intracellular DMSP concentrations. HTCC1062 cell suspensions were incubated under the same condition as in A). Negative controls were killed cell cultures. 1 µM DMSP was added at T=0 to cells that had been grown in the absence of DMSP, and 10 mL aliquots were filtered through 0.1 µm membranes at different time points to retain the cells. The intracellular DMSP concentrations were quantified by measuring DMS release after hydrolysis in NaOH. Results are the average of triplicate samples and error bars show the standard deviation (n=3).

Figure 3. DMSP catabolic pathways and homologs identified in the HTCC1062. Predicted enzymes in the cleavage pathway are in red, enzymes in the demethylation pathway are in green. Proteins in black indicate that no homologs were identified in the HTCC1062. The distributions of these pathways across the *Pelagibacterales* is described in more detail in Figures S1 and S5.

Tables

Table 1. Mass balance calculated from Figure 1A.

	Concentration (nM)	%
Δ DMSP	- 122	100%
Δ DMS	+ 73	59%
Δ MeSH	+ 26	21%
Δ Cellular sulfur[a]	+ 1	1%
Missing sulfur[b]		19%

[a]Estimated cellular sulfur demands according to the previous study[10].

[b]The DMSP loss unaccounted for could be due to measurement errors, oxidation of MeSH, or DMSP accumulation within cells.

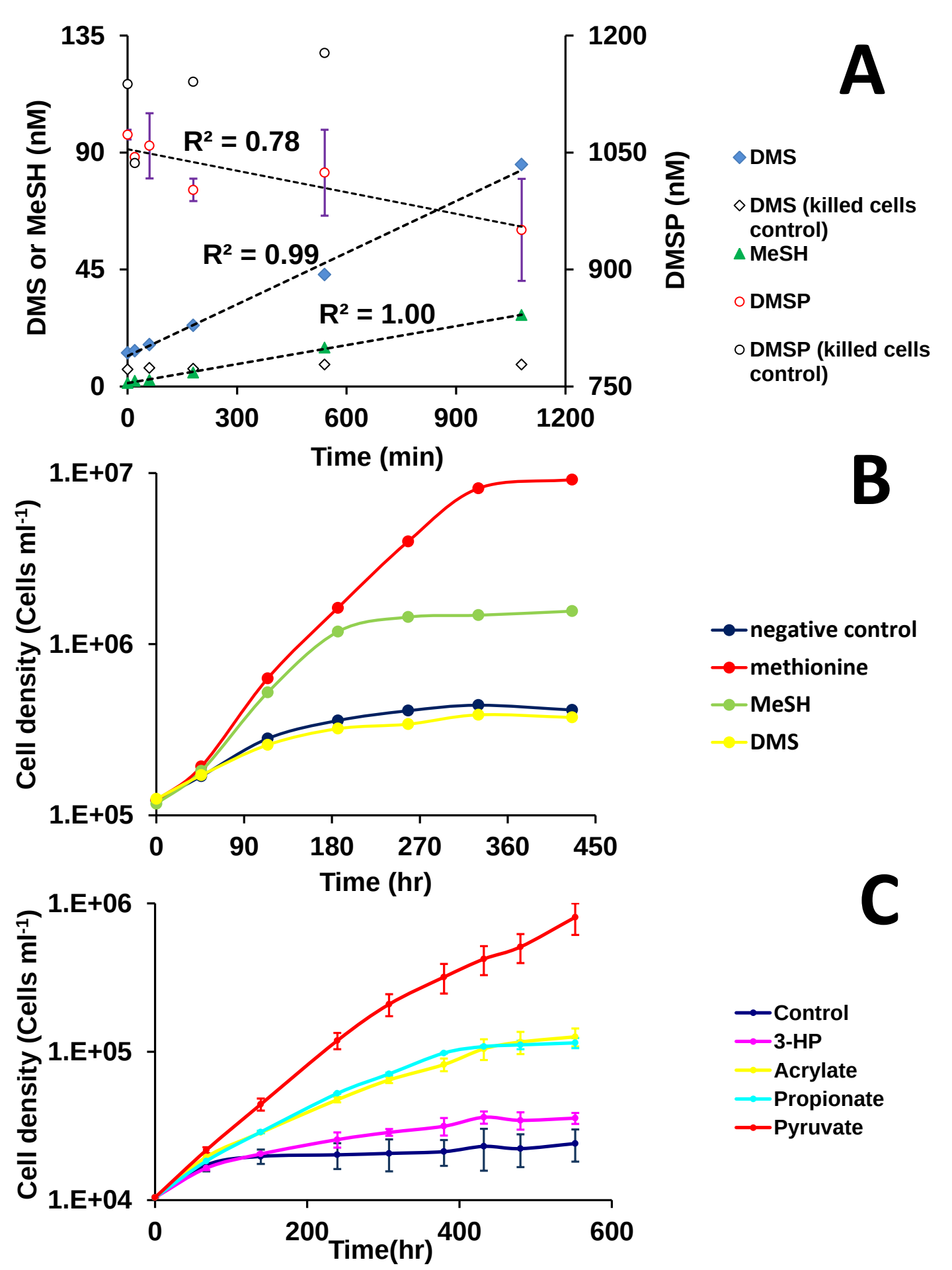
A
135
90
45
0
1200
1050
900
750
DMS or MeSH (nM)
DMSP (nM)
R² = 0.78
R² = 0.99
R² = 1.00
0
300
600
900
1200
Time (min)
DMS
DMS (killed cells control)
MeSH
DMSP
DMSP (killed cells control)
B
1.E+07
1.E+06
1.E+05
Cell density (Cells ml-1)
0
90
180
270
360
450
Time (hr)
negative control
methionine
MeSH
DMS
C
1.E+06
1.E+05
1.E+04
Cell density (Cells ml-1)
0
200
400
600
Time(hr)
Control
3-HP
Acrylate
Propionate
Pyruvate

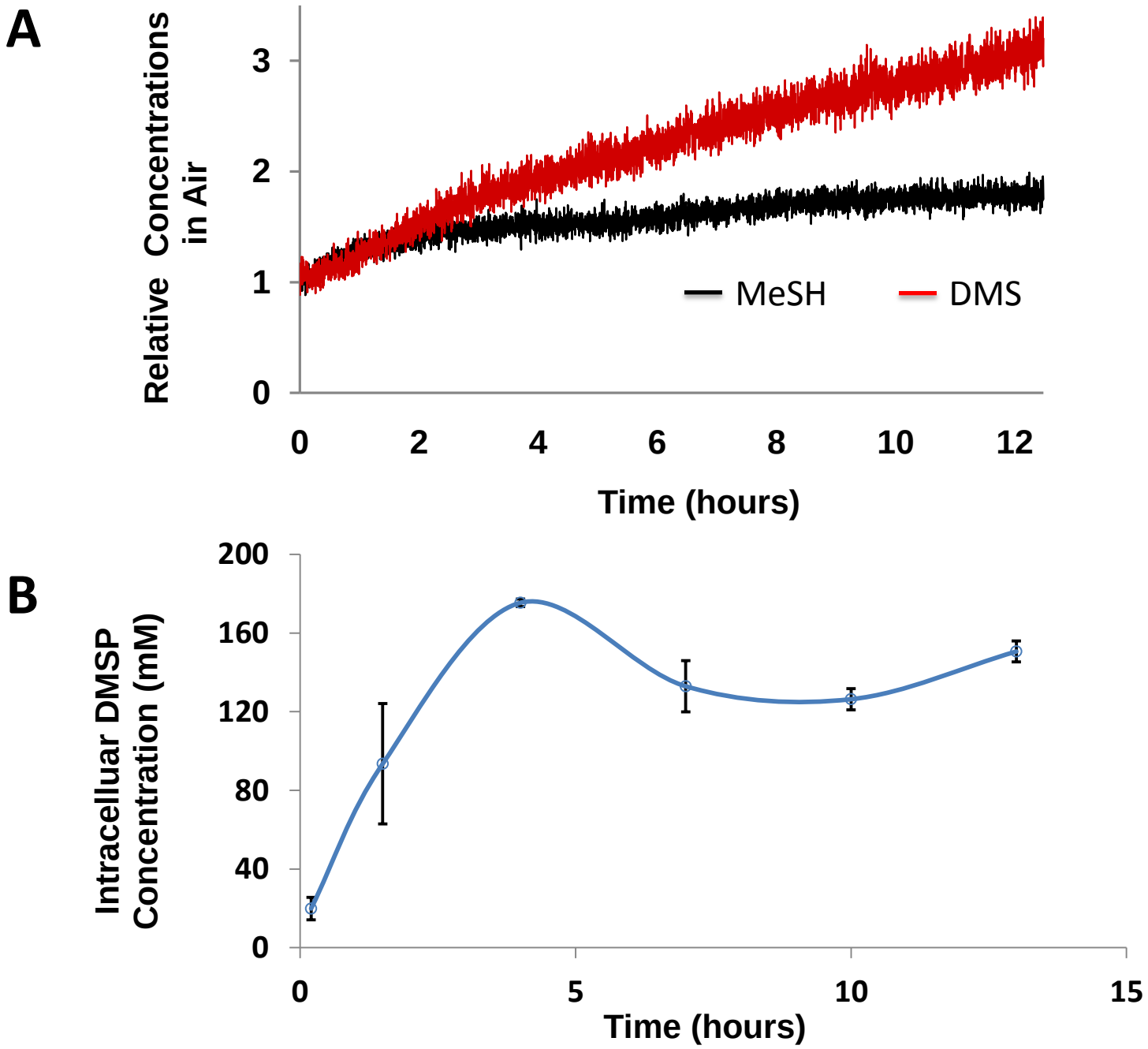
A
Relative Concentrations in Air
3
2
1
0
MeSH
DMS
0
2
4
6
8
10
12
Time (hours)
B
Intracelluar DMSP Concentration (mM)
200
160
120
80
40
0
0
5
10
15
Time (hours)

Supplementary Information

Jing Sun[1], Jonathan D. Todd[4], J. Cameron Thrash[5], Yanping Qian[2], Michael C. Qian[2], Ben Temperton[6], Jiazhen Guo[7], Emily K. Fowler[4], Joshua T. Aldrich[8], Carrie D. Nicora[8], Mary S. Lipton[8], Richard D. Smith[8], Patrick De Leenheer[3], Samuel H Payne[8], Andrew W. B. Johnston[4] Cleo L. Davie-Martin[1], Kimberly H. Halsey[1] and Stephen J. Giovannoni[1]*

[1]Department of Microbiology, [2]Department of Food Science, [3]Department of Mathematics, Oregon State University, Corvallis, Oregon 97331, USA; [4]School of Biological Sciences, University of East Anglia, Norwich Research Park, Norwich, NR4 7TJ, UK; [5]Department of Biological Sciences, Louisiana State University, Baton Rouge, LA, 70803, USA; [6]Plymouth Marine Laboratory, Prospect Pl, Plymouth, Devon PL1 3DH, UK. [7]Qingdao Aquarium, Qingdao, Shandong 266003, China. [8]Environmental Molecular Sciences Laboratory, Pacific Northwest National Laboratory, Richland, WA, 99352, USA.

Contents:

Supplementary Note I: DMSP catabolic pathways in *Pelagibacterales*.

Figure S1 shows DMSP catabolic pathways in diagrammatic form. Genes that are predicted to encode enzymes for the metabolism of acrylate were present in most *Pelagibacterales* strains. Acrylate can be metabolized to 3-hydroxypropionate (3-HP) by the action of AcuNK[1]. However, while AcuK is found in all strains, AcuN is not a core gene among the *Pelagibacterales*. 3-HP can be oxidized to an intermediate, malonate semialdehyde (mal-SA) and then acetyl-CoA, by an alcohol dehydrogenase (DddA) and mal-SA dehydrogenase (DddC), respectively. The predicted homologs for both *dddA* and *dddC* are found in all *Pelagibacterales* strains. *yhdH* is a homolog of *acuI* that recently was implicated in reductive 3-HP metabolism in *Rhodobacter sphaeroides* and *R. pomeroyi,* and was proposed as part of a novel pathway that converts acrylate to propionyl-CoA via acrylyl-CoA in those organisms [2,3]. This gene has homologs in all *Pelagibacterales* strains except HIMB59. The enzyme that converts acrylate to acrylyl-CoA has recently been identified as a propionate-CoA ligase (PrpE) in *R. pomeroyi*[4]. PrpE carries out multiple functions, and is involved in a third pathway for acrylate degradation via transformation to propionate and propionyl-CoA by acrylate reductase and PrpE, respectively. Acrylate reductase is missing from *Pelagibacterales*, but PrpE is present in all strains.

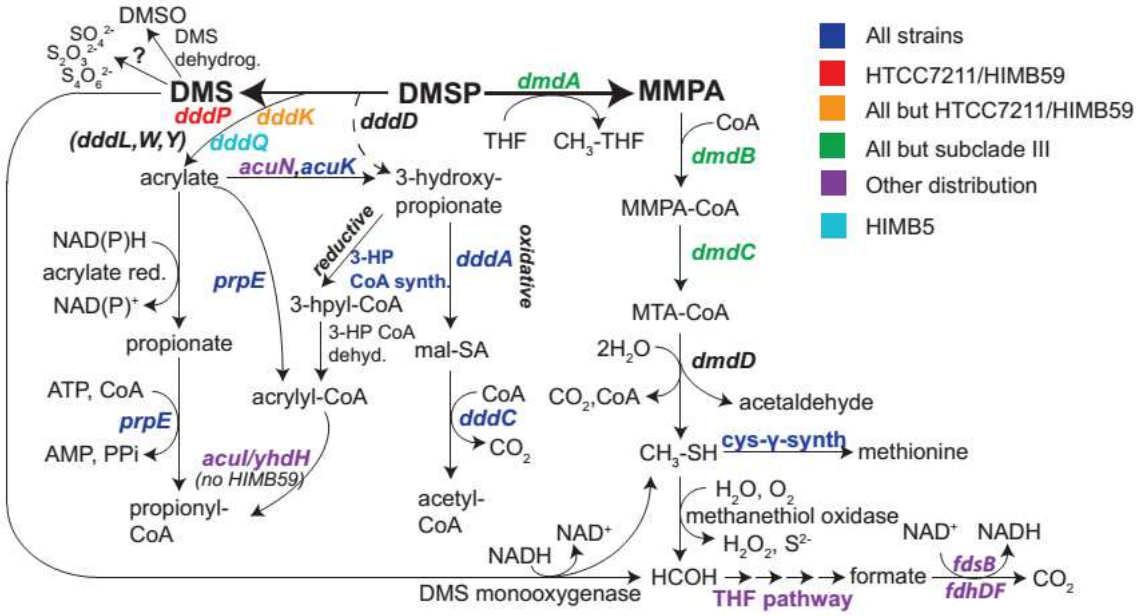

Figure S1. DMSP catabolic pathways and homologs identified in *Pelagibacterales* genomes. The dashed line indicates a proposed pathway. Question marks indicate unknown enzymes. All strains belonging to the temperate ocean surface type Ia.1 have *dddK*, but most strains from subtropical ocean sites, type Ia.3, have *dddP,* or *dddQ* (HIMB5) (Fig.S5). Genes in black did not have identified homologs in *Pelagibacterales*. In the western Sargasso Sea, type IIIa is found in surface waters in the fall. HIMB59, a type V isolated from the subtropical Pacific, represents an early branch of *Pelagibacterales*[5].

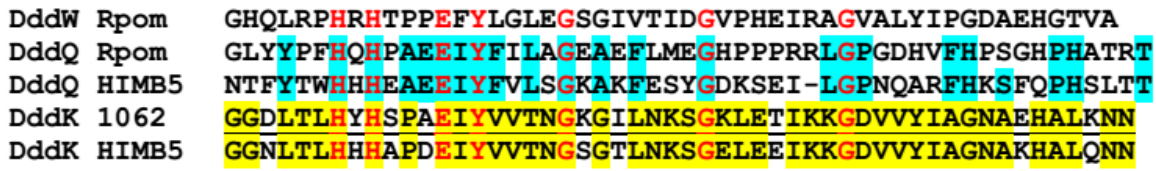

Figure S2. Comparison of *Pelagibacterales* DddK and DddQ-like polypeptides with other cupin DMSP lyases. The amino acid sequences of the cupin domains of the known DddW and DddQ polypeptides in *R. pomeroyi* are lined up in comparison with the DddK polypeptides of *Pelagibacterales* strains HTCC1062 and HIMB5 (gene products SAR11_0394 and HIMB5_00004730, respectively) and the DddQ-like product of the HIMB5_00000220 gene of *Pelagibacterales* strain HIMB5. Residues conserved in all polypeptides are shown as red letters. Yellow shading denotes identical residues in the two DddK polypeptides and turquoise shading shows those residues in common in the DddQs of *Pelagibacterales* HIMB5 and of *R. pomeroyi.*

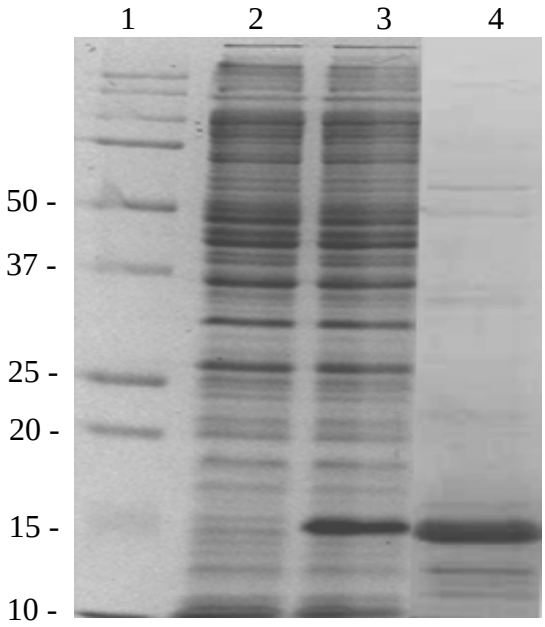

Figure S3: Stained SDS-PAGE image showing partial purification of histidine-tagged DddK (SAR11_0394). His-DddK has a predicted molecular mass of 15.8 kDa. Lane 1 = Precision Plus Protein Dual Colour Standards (Biorad); Lane 2 = soluble fraction of wild type *E. coli* BL21; Lane 3 = Soluble fraction of BL21 containing cloned *dddK* in pBIO2206; Lane 4 = DddK-containing sample used for kinetics determinations. 0.1% SDS-PAGE gels prepared with a 15% acrylamide resolving gel, topped with a 6% stacking gel. Loaded samples 1 and 2 are ~2.5 µg and the purified protein sample in Lane 4 was ~250 ng. Gels were run in vertical tanks (ATTO AE-6450) at 150 V for 2 hours in PAGE running buffer [25 mM Tris, 200 mM glycine, 0.1% SDS (w/v)]. Gels were stained with InstantBlue™ (Expedeon). Purity of DddK is 76%, which was determined by gel densitometry using *ImageJ***.**

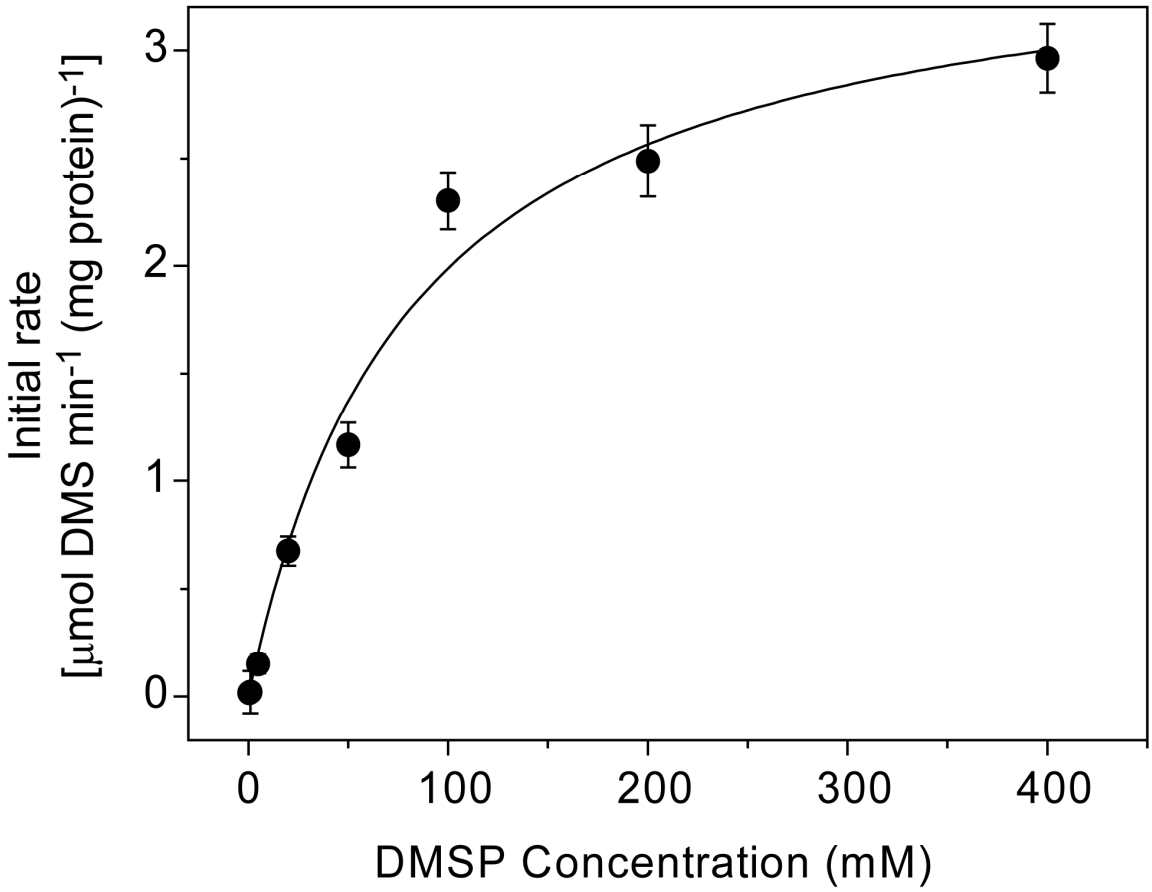

Figure S4. Kinetic analysis of enzyme activity. Michaelis-Menten plot for the DMSP lyase activity of DddK (SAR11_0394). For kinetics analysis of DddK initial rates were fitted to the Michaelis-Menten equation using *Origin* software (version 8, Origin Labs). V_{max} was calculated as 3.61 ± 0.27 µmol DMS min^{-1}(mg protein)$^{-1}$, and K_m 81.9 ± 17.2 mM DMSP. DddK (1.2 µg) was in sodium phosphate buffer (pH 8.0.). The R^2 value for the fit is 0.982. Standards errors are indicated (n=3).

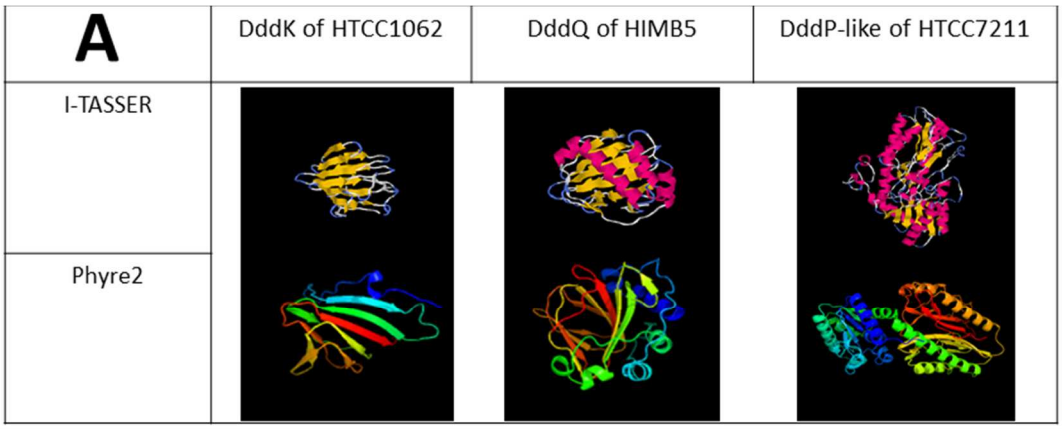

B

	***Pelagibacterales* strains**														
	Ia.1						Ia.3					Ia-	IIIa		V
	HTCC 1062 (OC)	HTCC 1002 (OC)	HTCC 1013 (OC)	HTCC 1016 (OC)	HTCC 1040 (OC)	HTCC 9565 (OC)	HTCC 9022 (OC)	HTCC 7211 (SS)	HTCC 7214 (SS)	HTCC 7217 (SS)	HTCC 8051 (OC)	HIMB 5	HIMB 114	IMCC 9063	HIMB 59
DddK	+	+ (97% Ident[a])	+ (73% Ident[a])	+ (98% Ident[a])	+ (98% Ident[a])	+ (89% Ident[a])	+ (89% Ident[a])	-	-	-	-	+ (73% Ident[a])	- (28% Ident[a])	- (26% Ident[a])	-
DddQ	-	-	-	-	-	-	-	-	+ (43% Ident[b])	-	-	+	-	-	-
DddP-like	-	-	-	-	-	-	-	+	+ (99% Ident[c])	+ (98% Ident[c])	-	-	-	-	+ (47% Ident[c])

[a], the identity to the DddK of HTCC1062. [b], the identity to the DddQ of HIMB5. [c], the identity to the DddP-like of HTCC7211.

Figure S5. Evolutionary relationships among *Pelagibacterales* DMSP lyases. An analysis of relationships among the SAR11 lyases we report on was done using BLASTP, protein structural prediction programs (I-TASSER, Phyre2) and SFams protein database[6]. **A)** Predicted protein structures of DddK from HTCC1062, DddQ from HIMB5 and DddP-like protein from HTCC7211 by I-TASSER and Phyre2. DddK, DddQ and DddP-like protein appear to belong to different protein families, although DddK and DddQ both have predicted cupin domains, and may belong to the same superfamily. Comparison of DddK, DddQ and DddP-like protein to the SFam database of hidden Markov models showed that each protein was recruited to a separate SFam model. Furthermore, the top-hitting family for each sequence was additionally found to be included in a separate 'clan' from the others (as defined by the 'precision 80' set of clans provided by SFam; families that reciprocally recruit at least 80% of each other's sequences are placed into a clan together). There is no evidence to show that these three proteins are evolutionarily related, which favors the explanation that these proteins are non-orthologous. **B)** The distribution of DMSP lyase families in *Pelagibacterales* strains. '**+**' means the homolog of DMSP lyase is present. '**-**' means the homolog of DMSP lyase is missing. 'OC' indicates strains that were isolated from the Oregon coast. 'SS' indicates strains that were isolated from the Sargasso Sea. The proteins that have been tested for DMSP lyase activity are squared in red.

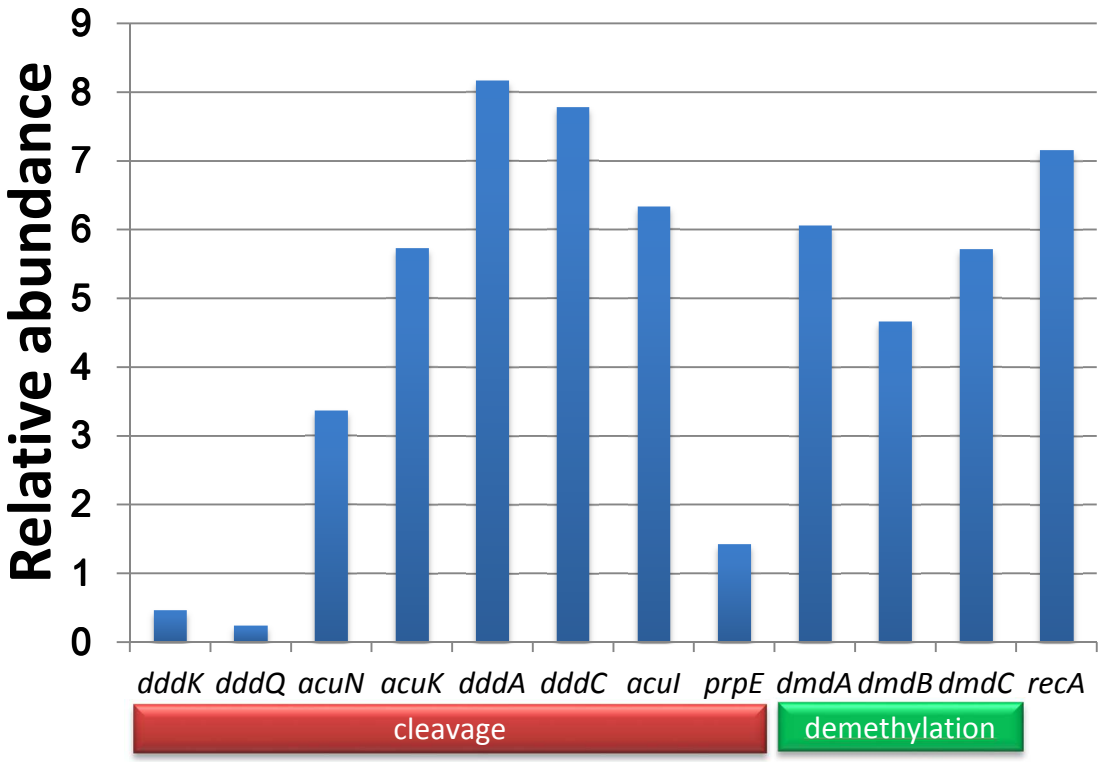

Figure S6. The relative abundance of *Pelagibacterales* DMSP catabolism genes in the GOS dataset. Genes were identified as *Pelagibacterales* clades by a reciprocal best BLAST (RBB) approach. For each gene, the count of hits was normalized by gene length, and the normalized values were summed across species. The frequency of the single copy *recA* gene was used to evaluate the abundance of the DMSP metabolism genes.

Supplementary Note II: Transcriptional and proteomic analysis of the DMSP metabolic pathways in *Pelagibacterales* strain HTCC1062.

To determine whether DMSP catabolic pathways are regulated in HTCC1062, we first examined changes in transcription in response to the addition of DMSP to the growth medium. Briefly, HTCC1062 cells were grown in autoclaved, filtered artificial seawater (ASW) media (1 mM NH_4Cl, 100 μM KH_2PO_4, 1 μM $FeCl_3$, 80 μM pyruvate, 40 μM oxaloacetate, 40 μM taurine, 50 μM glycine, 50 μM methionine and excess vitamins[7]) in the presence and absence of 1 μM DMSP. Changes in transcription were measured with Affymetrix GeneChip oligonucleotide microarrays (Microarray data was deposited in GEO (GSE65845)), as described in a previous publication from our research group[8]. Differences were deemed significant when genes exhibited either a 2-fold change or greater between treatments and controls, and when the fold change value indicating differential expression was supported by a Q-value of 0.05 or less (data not shown). No significant changes were observed in the expression of genes involved in DMSP metabolism (e.g., the genes in Fig. S6), including *dddK* and *dmdA* genes, indicating that these genes and pathways are not transcriptionally regulated.

Because transcriptional analysis reveals changes in transcription, but not whether genes are expressed and translated, we applied quantitative proteomics using the isobaric tag for relative and absolute quantitation (iTRAQ) method to compare DMSP catabolic pathway proteins in cells grown in the presence and absence of DMSP. All proteins involved in DMSP metabolic pathways (AcuIK, DddAC, PreE, DmdABC) were detected, except DddK. The absence of DddK does not show that it is not present, but rather is likely an unfortunate consequence of DddK not producing detectable peptides in the iTRAQ experiments. The DddK peptide sequence exhibits an unusually small number of tryptic peptides that are predicted to produce MS/MS spectra. Studying data from many other experiments, we found that one peptide that likely originates from DddK was frequently detected in cells grown under a variety of conditions, but, since we don't score any protein as 'detected' unless two peptides are observed, DddK is marked as 'unobserved' in all of our work. In the iTRAQ experiments not even this single DddK peptide was observed; while unfortunate, this is not surprising because iTRAQ experiments have unique biases associated with peptide chemistry that can cause additional peptides to be missed.

In accord with the transcription data, the iTRAQ experiment revealed few significant changes in the abundance of proteins for DMSP metabolism (Figure S7; Table S2). Two proteins in the predicted pathways of DMSP cleavage and demethylation were among the significantly differentially abundant proteins, but the changes in protein abundance were small: DmdC was 25% more abundant in cultures amended with DMSP than in those amended with methionine, and DddC was 20% more abundant in cultures amended with methionine than those amended with DMSP.

To summarize, the microarray and iTRAQ data collectively provide compelling evidence that both pathways for DMSP catabolism are constitutively produced by HTCC1062 cells, whether DMSP is present in the medium or not.

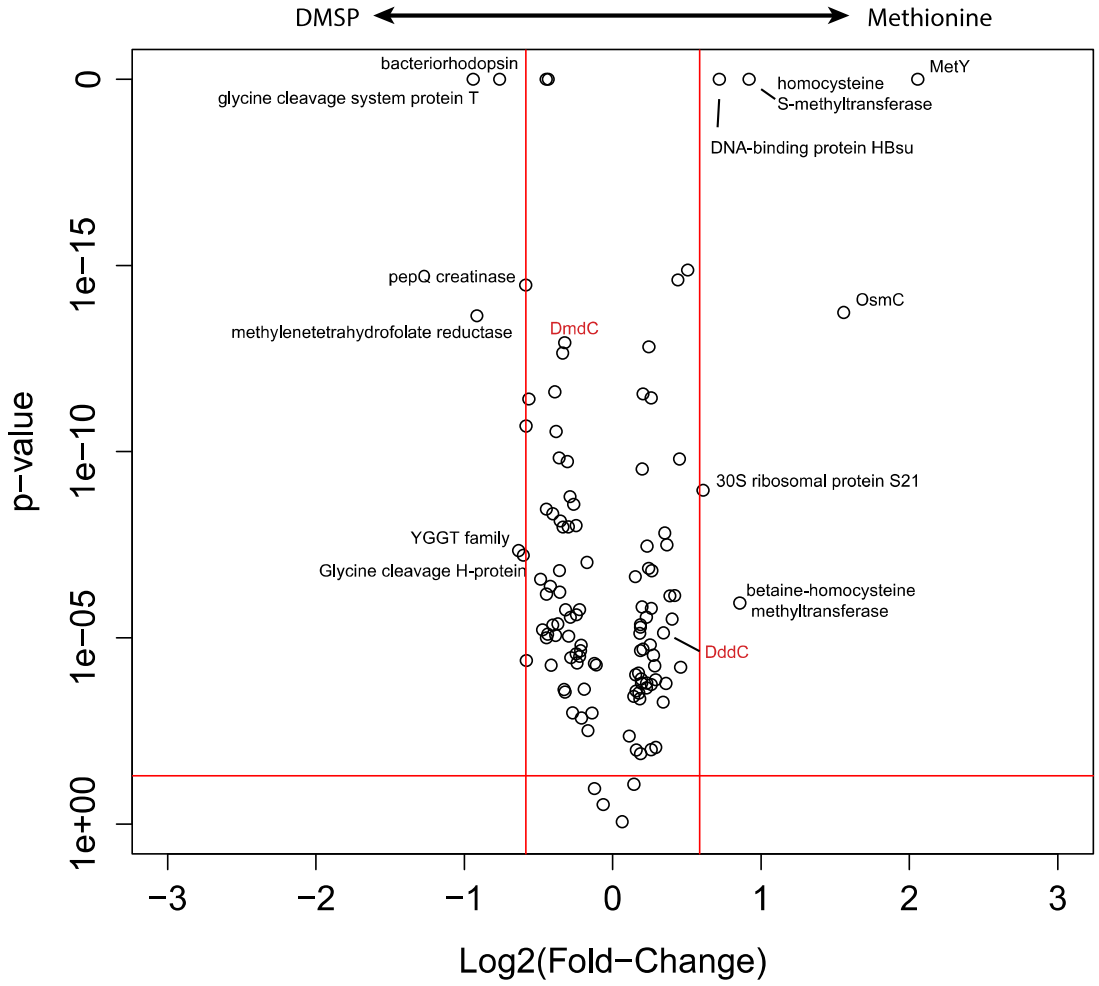

Figure S7. Volcano Plot of differential protein expression between HTCC1062 cultures amended with DMSP (left) vs. cultures amended with methionine (right) as determined by quantitative iTRAQ proteomics. Horizontal red line indicates a p-value cut-off of 0.05; Vertical red lines indicate boundaries of 1.5-fold difference in expression.

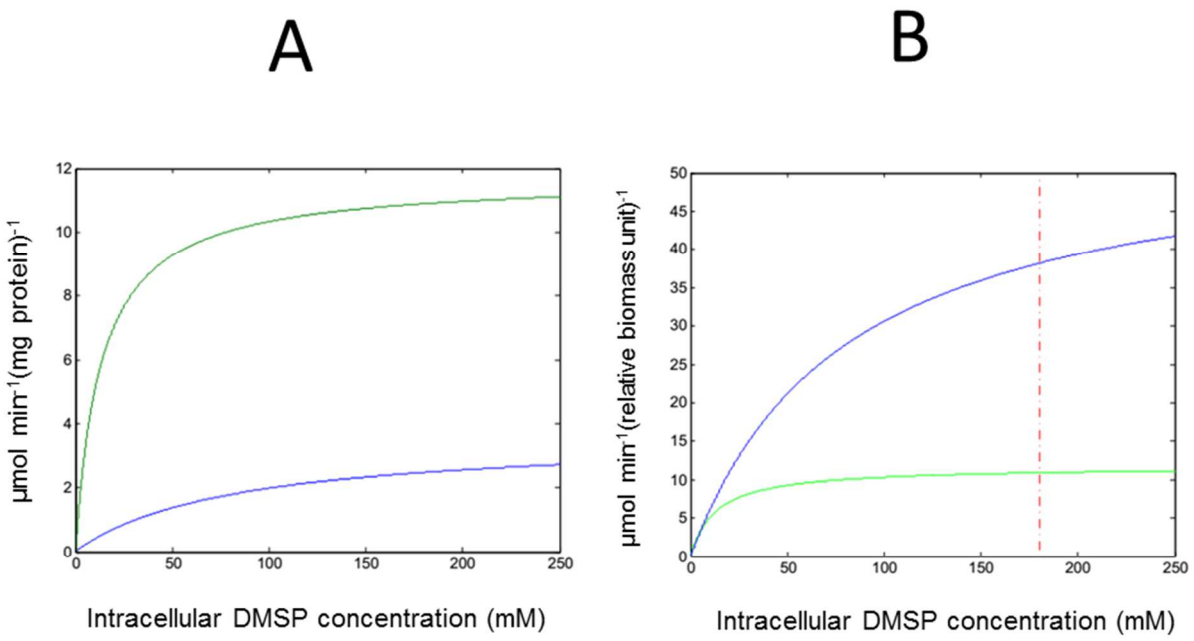

Figure S8. Kinetic models for DMS and MeSH production as a function of intracellular DMSP concentration. A) Product formation rates modeled as $dP_1/dt = V_{m1}S/(S+K_{m1})$ for MeSH formation by DmdA (green) and modeled as $dP_2/dt = V_{m2}S/(S+K_{m2})$ for DMS formation by DddK (blue). Parameter values: V_{m1} = 11.7 µmol min^{-1} mg^{-1}, K_{m1} = 13.2 mM, V_{m2} = 3.6 µmol min^{-1} mg^{-1}, K_{m2} = 81 mM. Note that the model in Fig. S8A does not fit the observations shown in Fig. 1A, but this is not a surprise because the model shown in Fig. S8A assumes equivalent amounts of the two enzymes, DddK and DmdA. **B)** To solve for rates of production of DMS and MeSH that match the observations shown in Fig. 1A, we assumed an intracellular DMSP concentration of 180 mM, and adjusted activities such that the amount (by weight) of DddK (15.8 kDa) is X-fold (F=15) DmdA (~40kDa), yielding the model seen in Fig. S8B.

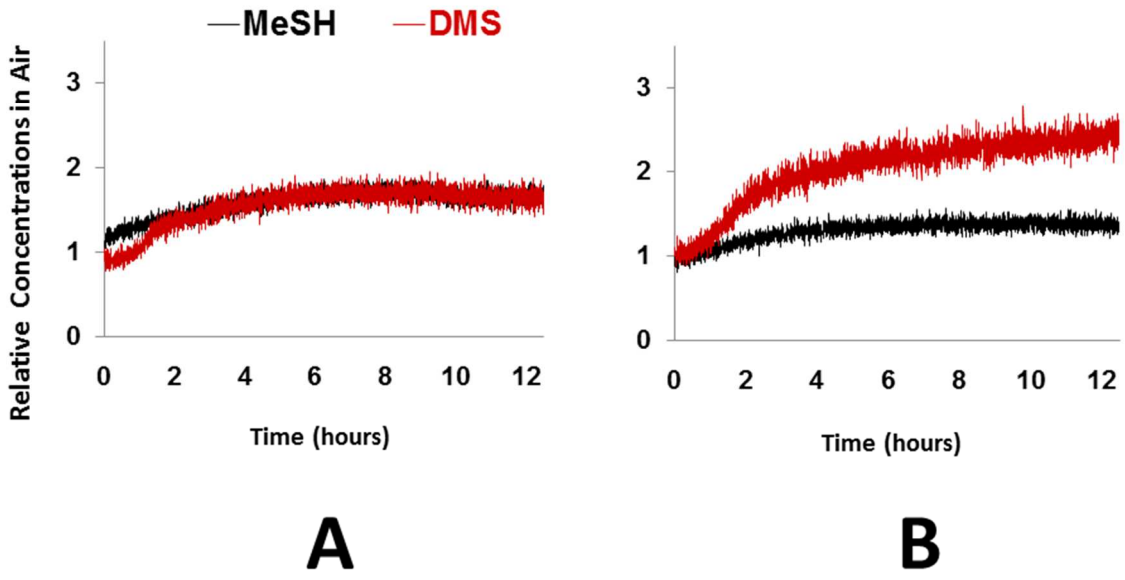

Figure S9. Real-time gas-phase MeSH and DMS production measurements by PTR-TOF/MS. The data in panel A and B are from experiments similar to Fig. 2A. This experiment was repeated three times. The second and the third repeats are shown here. HTCC1062 cell suspensions were incubated in ASW and subjected to a flow of fine bubbles. DMSP was added at T=0 to cells that had been grown in the absence of DMSP. Measurements are presented in relative concentration units and were normalized to the gas-phase concentrations of MeSH and DMS (m/z 49 and 63, respectively) at T=0.

Supplementary Note III: Enzymatic activities of DddKs in *Pelagibacterales* strains.

DddK homologs from strains HTCC9022 and HMIB5 were cloned and expressed, and as expected the *E. coli* transformants showed DMSP lyase activities similar to that observed in the original DddK from strain HTCC1062 (Table S1). We also tested the most distant DddK-like proteins of strains HIMB114 (28% identity) and IMCC9063 (26% identity) from *Pelagibacterales* IIIa subclade[9]. However, the cloned genes from these strains had no DMSP lyase activity (were similar to *E. coli* with the empty vector).

Table S1. Enzymatic activities of DddK proteins from a variety of *Pelagibacterales* strains

***Pelagibacterales* strain**	**DMS production (μmol min^{-1} mg^{-1})**
803 pUC57 (*E. coli*: empty vector)	0.013 ± 0.000
HTCC1062 (YP_265818)	1.233 ± 0.087
HIMB5 (WP_014953073)	0.588 ± 0.114
HTCC9022 (WP_028037226)	0.975 ± 0.041
HIMB114 (WP_009359929)	0.013 ± 0.003
IMCC9063 (WP_013695448)	0.011 ± 0.000

Supplementary Note IV:

Twelve proteins were identified as having a differential expression of > 1.5-fold between DMSP and methionine treatments (Figure S7; Table S2). As MetF catalyzes the conversion of CH_3-THF to CH_2-THF, up-regulation of MetF in the presence of DMSP is consistent with increased concentrations of CH_3-THF resulting from conversion of DMSP to MMPA by DmdA. Similarly, GcvT is required alongside FolD in the conversion of CH_2-THF to CHO-THF. SAR11_1724 is a protein of unknown function containing a YGGT domain conserved among integral membrane proteins of unknown function.

Quantitative proteomics provided evidence of up-regulation of PepQ (SAR11_0687) in the presence of DMSP. As structurally similar creatinases have previously been found to have DMSP lyase activity[10], SAR11_0687 was synthesized, cloned and overexpressed in *E. coli* as described previously. However, SAR11_0687 showed no evidence of DMSP lyase activity (data not shown), therefore it is unlikely that this protein is responsible for DMSP cleavage in HTCC1062.

Table S2. Proteins with differential expression > 1.5-fold between HTCC1062 cultures amended with methionine vs. cultures amended with DMSP as determined by quantitative iTRAQ proteomics. Fold change was calculated using the LIBRA module of the Trans-Proteomic Pipeline and by linear mixed-effects model encompassing a fixed treatment effect and random effect for each peptide associated with the protein. Bold-text indicates proteins enriched in DMSP amended cultures.

Locus	Protein	Coverage* (%±1 s.d.)	LIBRA fold change (Met/DMSP)	Lmer fold change (Met/DMSP)
SAR11_1030	MetY	60.6 ± 0.8	3.46	4.12
SAR11_0750	homocysteine S-methyltransferase	30.9 ± 2.5	1.88	1.89
SAR11_0817	non-specific DNA-binding protein HBsu	76.5 ± 0.6	1.06	1.65
SAR11_1172	OsmC	50.6 ± 12.7	2.74	2.94
SAR11_1173	betaine-homocysteine methyltransferase	36.3 ± 1.4	1.82	1.81
SAR11_0578	30S ribosomal protein S21	55.7 ± 6.3	1.15	1.52
SAR11_0625	**proteorhodopsin**	**17.0 ± 3.9**	**0.59**	**0.59**
SAR11_0687	**pepQ creatinase**	**23.8 ± 4.2**	**0.66**	**0.67**
SAR11_0667	**GcvH glycine cleavage H-protein**	**26.5 ± 3.2**	**NA**	**0.66**
SAR11_1264	**MetF methylenetetrahydrofolate reductase**	**28.7 ± 6.8**	**0.57**	**0.53**
SAR11_1265	**GcvT glycine cleavage system protein T**	**34.7 ± 5.2**	**0.43**	**0.52**
SAR11_1724	**YGGT family**	**13.6 ± 0.0**	**0.63**	**0.64**

*Coverage of the total protein length by peptides with a PeptideProphet probability > 0.95

Supplementary Note V: DMSP transport

It is reasonable to propose that *Pelagibacter* cells can concentrate DMSP from the environment, where ambient concentrations are ~ 2 nM (Table S3), to an intracellular DMSP concentration of greater ~ 180 mM (a concentration of 10^8 fold). Firstly, the transporter in question (OpuAC) was the sixth most highly detected *Pelagibacterales* protein in our study of the Sargasso Sea metaproteome[11], and one of the most highly detected proteins in cultured *Pelagibacter* proteomes. This transporter, which is often annotated as a glycine betaine transporter, is likely responsible for Kiene's observation that in seawater there is an abundant glycine betaine transporter that has a 5 nM half saturation constant and is competitively inhibited by DMSP[12]. Kiene wisely concluded that this is likely a multifunctional transporter that transports DMSP[12]. Note that *Pelagibacter* has been proven to transport both glycine betaine and DMSP, and has a single ABC transporter of the appropriate type. Thus, everything we report here is consistent with published knowledge on this topic.

In addition, it is also a reasonable prediction from thermodynamics. For active transport from 2 nM to 200 mM:

$$\Delta G = 2.303\ RT\ log10\ (10^{-9} \div 10^{-1})$$

= 10.9 kcal $mole^{-1}$

Since the transporter in question is an ABC transporter that relies on ATP hydrolysis, -12 kcal mol^{-1} is available.

The cytoplasmic volume of *Pelagibacter* cells (the same strain used in our paper about DMSP) was at ~0.01 μm^3 [13]. At an internal concentration of 200 mM, the amount of DMSP inside a cell would be (1×10^{-17} liters $\times$ 0.2 M) 2×10^{-18} moles DMSP/cell. This number is consistent with what is known about the biology of the smallest cells. Assuming a spherical cell, the estimated diameter of the cytoplasmic volume is ~0.12 µm.

To calculate flux, assume

$$Flux = 4\pi DRC_{\infty}$$

where *R* is the radius

D is the diffusion coefficient

C is the ambient concentration in the fluid

Assuming a D of 10^{-9} m^2 sec^{-1} (perhaps a slight overestimate) with an R of 0.06 µm

Then 1.5 x 10^{-21} moles DMSP per cell $\times$ sec^{-1}

Thus, without factoring in catabolism, it would take ~1300 seconds, or ~22 minutes, to accumulate DMSP to 200 mM, based on the laws of diffusion, active transport, and the assumption of 2 nM ambient DMSP.

Table S3: Concentrations of dissolved DMSP (DMSPd) in the Oceans as reported in the literature.

DMSPd concentration	location	References
10-100 nM	Antarctic coastal waters	14
1-34 nM	Wadden Sea	15
1.1 - 15 nM	Mauritanian upwelling regions	16

Up to 6 nM	Monterey Bay, CA	17
0.1 nM to 11 nM	Northern Gulf of Mexico	18*
1-10 nM	Gulf of Mexico mesotrophic shelf	19*
0.2 – 2.6 nM	Gulf of Mexico oligotrophic oceanic	
5.6 -198.8 nM (180-6360 ng S/L)	The North Sea and English Channel	20*
65 nM	The Bay of Villefrance-sur-mer	21*
2 - 9 nM	Sargasso Sea	22*
2.5 – 11.4 nM	Vineyard Sound, Massachuset	
Up to 30 nM	Delaware Bay	23*
3nM	Western Mediterranean waters	24*
4 - 150 nM	The North Sea	25*
1 - 1.6 nM	Mediterranean	
1.1 – 24 nM	The North Atlantic	

*These measurements were made before Kiene et al.[26] reported that DMSPd concentration measurements can be influenced by filtration artifacts.

Table S4. Accession numbers used in Fig. 3 and Fig. S1. This table is provided as a separate file.

Supplementary Methods:

Synthesis and cloning of *Pelagibacterales ddd* genes that encode DMSP lyases

The intact *dddK* genes from SAR11 strains HTCC1062 (SAR11_0394); HTCC9022 (no gene tag available), HIMB5 (HIMB5_00004730); and *dddK*-like genes from *Pelagibacterales* strains HIMB114 (no gene tag) and IMCC9063 (SAR11G3_00808); and *dddQ* from strain HIMB5 (HIMB5_00000220) were each synthesized with codon usage being optimised for expression in *E. coli*. The genes were provided cloned into pUC57 containing the engineered ribosome binding site sequences "TCTAGAAATAATTTTGTTTAACTTTAAG**AAGGAG**ATATACAT**ATG**" (from pET21) incorporated directly upstream of their ATG start codons. These recombinant plasmids were each transformed into *E. coli* 803 on LB media containing 100 µg mL^{-1} ampicillin and assayed for DMSP lyase activity, as described below.

The *dddK* and *dddQ* genes of strains HTCC1062 and HIMB5 respectively were then sub-cloned into the expression vector pET16b using *Nde*I and *Bam*HI, and the resulting plasmids were each transformed into competent *E. coli* BL21 on LB media containing ampicillin. Transformants were used for protein purification, taking advantage of the His tag, which is incorporated into pET16a-based recombinant plasmids.

Assays of DMSP lyase

E. coli 803 or BL21 strains containing cloned *ddd* genes cloned in pUC57 or pET16b, respectively or with the vectors alone, were grown at 37°C in 5 mL of LB broth containing ampicillin (100 µg mL^{-1}) to an OD_{600} of 0.8. The cells were diluted 10-fold into 300 µL M9 media containing 1 or 5mM DMSP and 100 nM IPTG for pET16b clones in 2 mL vials (Alltech Associates). Vials were incubated at 28°C for 18 hours and the concentrations of DMS in the headspace were measured by gas chromatography, using a flame photometric detector (Agilent 7890A GC fitted with a 7693 autosampler) and HP-INNOWax 30 m x 0.320 mm column (Agilent Technologies J&W Scientific) capillary column. The assayed cells were pelleted, re-suspended and washed three times in 1 mL of phosphate buffered saline pH 7.4, then lysed by sonication (6 × 10 s, full power) and the protein concentrations were estimated as described by Bradford[27].

Purification and characterization of DddK

A 50 mL culture of *E. coli* containing the recombinant plasmid in which *dddK* of strain HTCC1062 cloned in pET16b was grown in LB at 28ºC in the presence of 100 nM IPTG. The cells were harvested, pelleted and re-suspended in 1.4 mL NPI-10 buffer (50 mM sodium phosphate, 300 mM sodium chloride, 10 mM imidazole), then lysed by sonication (lane 3, Figure S4). The lysate was centrifuged at 13,000 RPM, and the soluble fraction was applied, in two loads of 0.7 mL, to a *Qiagen* Ni-NTA spin column. The column was washed three times with NPI-30 buffer (50 mM sodium phosphate, 300 mM sodium chloride, 30 mM imidazole). Then, the bound His-DddK was eluted at pH 8.0 using NPI-300 buffer (50 mM sodium phosphate, 300 mM NaCl, 300 mM imidazole), an aliquot of which is shown in Figure S4.

To determine the enzyme kinetics of DddK, 1.2 µg of the protein (76% pure) was added to 30 µL NPI-10 buffer (pH 8.0) containing varying DMSP concentrations, in sealed vials. Initial reaction rates were measured by assaying DMS in the headspace over a 30 minute incubation period at 22°C.

Nuclear magnetic resonance (NMR)

From a 5 mL culture of *E. coli* BL21, a 2 mL aliquot was re-suspended in 1 mL of 20 mM Tris:D_2O (pH 6.45). Cells were sonicated, the debris removed by centrifugation and the soluble fraction was incubated at 22°C for 1 h in the presence of 3 mM ^{13}C-DMSP[28]. 15 µL of 70% perchloric acid was added per mL^{-1} then incubated on ice for 15 min. NMR analysis of the sample was done as described in Todd *et al*[28].

Bioinformatics analysis and proposed DMSP metabolic pathways

We expanded on the knowledge obtained in Grote *et al*[5] by doing additional homology searches for DMSP metabolism genes using profile hidden markov models (HMMs)[29]. Because they are constructed with a range of probabilistic values for a given site in a protein, profile HMMs are superior to BLAST for finding distantly related homologs[30]. In this workflow, representative genes for the reactions in Fig. 3 and Fig. S1 were obtained from the original publications [3,31,32], searches of NCBI, and E.C. number searches based on figures from [1,33], and references therein (all starting sequence data is included in Table S4). These representative sequences were then searched against a database of profile HMMs created for over 436,000 protein families built with Markov clustering[9] using hmmscan from the HMMER3 package[34] on default settings. SFam HMMs with lowest expect values to the representative sequences were then searched against our *Pelagibacterales* genomes using hmmsearch on default settings. Homologs were classified based on HMMs having comparative expect values to both the representative sequence and a *Pelagibacterales* gene sequence.

Metagenomic analysis

To identify the relative abundance of *Pelagibacterales* genes involved in DMSP metabolism in surface water metagenomes, predicted proteins encoded by homologs of *acuIKN, dddACKPQ, dmdABC* and *prpE* were identified in all 14 genomes from the *Pelagibacter* clade (HTCC1002, HTCC1013, HTCC1062, HTCC7211, HIMB5, HIMB59, HIMB058, HIMB083, HIMB114, HIMB140, HTCC8051, HTCC9022, HTCC9565, IMCC9063) currently in the complete Integrated Microbial Genomes (IMG, http://img.jgi.doe.gov/) database (v. 400). Homologs were determined using a previously described comparative genomics analysis pipeline[5]. Genes within each cluster were used as queries in a TBLASTN (v. 2.2.22+) search against the Global Ocean Survey (GOS) nucleotide database available from CAMERA (http://camera.calit2.net/) with query filtering disabled and default *e*-value cutoff (-seg no –max_target_seqs 10000000). Nucleotide sequences returned from this search were used in a reciprocal best-BLAST (RBB)[35] filtering step against the amino acid sequences in the complete IMG database, returning the best hit to each nucleotide query (BLASTX, -max_target_seqs 1 –seg no). If the best hit for a nucleotide sequence in the RBB analysis was a protein sequence

from the original gene cluster, the nucleotide query was recorded as a successful hit; otherwise it was rejected. For each gene, the count of hits was normalized by gene length, and the normalized values were summed across species. The frequency of the single copy *recA* gene was used to evaluate the abundance of the DMSP metabolism genes.

Quantitative proteomics

HTCC1062 was grown in ASW amended with 100 μM NH_4Cl, 10 μM KH_2PO_4, 0.1 μM $FeCl_3$, 1 mM pyruvate, 500 μM glycine and excess vitamins[7]. Triplicate Samples were amended with 1 μM DMSP, or 1 μM methionine and samples with both 1 μM DMSP and 1 μM methionine are treated as positive controls. Cells were all harvested by centrifugation at the same time point in the exponential phase. Prior to harvesting, cultures were treated with chloramphenicol (0.01 g L^{-1}) and protease inhibitor cocktail Set II (0.1 mL L^{-1}, CalBiochem #539132). Cell pellets were immediately stored in - 80℃ prior to iTRAQ analysis at the Pacific Northwest National Laboratory (PNNL).

Each cell pellet was brought up to 100 μL with 8M urea (Sigma-Aldrich, St. Louis, MO) and sonicated in a water bath with ice until the pellet went into solution. The samples were briefly spun and transferred to PCT MicroTube barocycler pulse tubes with 150 μL caps (Pressure Biosciences Inc., South Easton, MA). The MicroTubes were placed in a MicroTube cartridge and barocycled for 10 cycles (20 s at 35,000 psi back down to ambient pressure for 10 s). All of the material was removed from the MicroTubes and transferred to 1.5 mL micro-centrifuge tubes. A Bicinchoninic acid (BCA) (ThermoScientic, Rockford, IL) assay was used to determine protein concentration. Dithiothreitol (DTT) was added to each sample at a concentration of 5 mM (Sigma-Aldrich, St. Louis, MO) and incubated at 60℃ for 1 h. The samples were then diluted 10-fold with 100 mM NH_4HCO_3, and tryptic digestion (Promega, Madison, WI) was performed at a 1:50 (w/w) ratio with the addition of 1 mM $CaCl_2$ to stabilize the trypsin and reduce autolysis. The sample was incubated for 3 h and cleaned via C-18 solid phase extraction (SPE) (Supelco, Bellefonte, PA) on a Gilson GX-274 ASPEC automated SPE system (Gilson Inc., Middleton, WI). The samples were dried to 50 μL and assayed with a Direct Detect IR Spectrometer (EMD Millipore, Billerica, MA) to determine the final peptide concentration.

Each sample set of 3 along with the pooled sample was dried in a speed-vac until near dryness and brought up to 30 μL with 1M Triethylammonium bicarbonate buffer (TEAB). Each sample was isobarically labeled using iTRAQ Multiplex (4-plex) Kits (ABsciex, Framingham, MA) according to the manufactures instructions. Briefly, 50 μL of isopropanol was added to each reagent (iTRAQ 114-117), vortexed and allowed to dissolve for 5 min with occasional vortexing. Reagents were then added to the samples, vortexed and incubated for 1 h at room temperature. The reaction was quenched by adding 100 μL of water to the sample with incubation for 15 min at room temperature. The samples within each set were then combined and dried in the speed vac to remove the organics. Each set was cleaned using Discovery C18 50 mg/1 mL solid phase extraction tubes as described above and once again assayed with BCA to determine the final peptide concentration. There were three technical replicates per sample.

Samples were diluted to a volume of 900 μL with 10 mm ammonium formate buffer (pH 10.0), and resolved on a XBridge C18, 250x4.6 mm, 5 μM with 4.6x20 mm guard column (Waters, Milford, MA). Separations were performed at 0.5 mL/min using an Agilent 1100 series HPLC system (Agilent Technologies, Santa Clara, CA) with mobile phases (A) 10 mM

ammonium formate, pH 10.0 and (B) 10 mM ammonium formate, pH 10.0/acetonitrile (10:90). The gradient was adjusted from at 100% A to 95% A over the first 10 min, 95% A to 65% A over minutes 10 to 70, 65% A to 30% A over minutes 70 to 85, maintained at 30% A over minutes 85 to 95, re-equilibrated with 100% A over minutes 95 to 105, and held at 100% A until minute 120. Fractions were collected every 1.25 min after the first 15 min (96 fractions). Every 12th fraction was then combined for a total of 12 samples (each with n=8 fractions pooled) for each of the 3 sets. All fractions were dried under vacuum and 20 µL of 25 mM ammonium bicarbonate was added to each fraction for storage at -20℃ until LC-MS/MS analysis.

Each iTRAQ run generated 152,8902345 spectra, identifying 1196 out of 1324 proteins in HTCC1062. Of these, 112 showed significantly different expression between DMSP and methionine treatments (methionine·$DMSP^{-1}$ fold-change median = 0.913, 1st quartile=0.783, 3rd quartile=1.19).

MS/MS datasets were searched against predicted proteins from *Ca.* P. ubique HTCC1062 using MSGF+ (http://proteomics.ucsd.edu/Software/MSGFPlus.html) with the following search parameters: dynamic methionine oxidation; partial trypsin digest; 20 ppm tolerance. Reporter ion intensities were collected using MASIC[36] and processed through the MAC (Multiple Analysis Chain) pipeline to aggregate, filter and generate cross-tabulated results for processing. Redundant peptide identifications had reporter ion intensities summed for a unique peptide result. Proteins were tested for significantly different expression between cultures grown on DMSP and those grown on methionine using a linear mixed-effects model below encompassing a fixed treatment effect and random effect for each peptide associated with the protein using the lme4 package in R:

$$
\begin{aligned}
y_{ij} &= \mu + b_i + p_j + \epsilon_{ijk} \\
p_j &\sim \mathcal{N}(0, \sigma_p^2) \\
\epsilon_{ijk} &\sim \mathcal{N}(0, \sigma^2) \\
i &= 1, ..., m \; j = 1, ..., n
\end{aligned}
$$

where μ is the intercept, b is the treatment effect, p is the random intercept associated with each peptide and ϵ is the per observation variation. The resulting linear model was tested for significance of the treatment fixed effect using ANOVA generating a p-value. The p-value was then adjusted for multiple comparisons using Benjamini-Hochberg p-value correction:

$$
\begin{aligned}
p.adj &= \frac{n}{Rank(pval)} pval \\
Rank(pval) &= \text{Rank of the p-value in the result set} \\
n &= \text{number of comparisons}
\end{aligned}
$$

Proteins with significantly different expression between DMSP and methionine treatments were verified with a complimentary analysis using the Trans-Proteomic Pipeline[37]. MS/MS spectra were searched against predicted proteins from HTCC1062 using X!Tandem with

identical parameters as before. Spectral matches were filtered using PeptideProphet ($p > 0.95$) and ProteinProphet ($p > 0.90$). Relative protein abundances were calculated using LIBRA using a default conditions file for 4-channel iTRAQ.

Linear regression showed that estimated fold-change size between lmer4 and LIBRA analyses for the 12 most differentially expressed proteins was highly correlated (coefficient=1.133 0.04 (s.e.), $R^2 = 0.99$, $F = 795.2$, d.f. = 10, $p = 7.31\times10^{-11}$) (SAR11_0667, the glycine cleavage H-protein was removed from the analysis as LIBRA failed to estimate relative abundances for this protein).

The mass spectrometry proteomics data have been deposited to the ProteomeXchange Consortium[38] via the PRIDE partner repository with the dataset identifier PXD001717.

DMSP model

Substrate competition model

Consider the following reaction scheme:

$$S + E_1 \longleftrightarrow C_1 \longrightarrow P_1 + E_1$$
$$S + E_2 \longleftrightarrow C_2 \longrightarrow P_2 + E_1$$

where *S*; E_1; E_2 and P_1; P_2 represent the concentrations of DMSP, demethylase, DMSP lyase, and MeSH, DMS respectively. The intermediate complexes are C_1 and C_2.

Assuming mass action kinetics, we can write the differential equations for the concentrations of the various compounds (the dots on the left hand side are shorthand for $d=dt$):

$$\begin{aligned}
\dot{S} &= -k_1 S E_1 - k_3 S E_2 + k_{-1} C_1 + k_{-3} C_2 \\
\dot{C}_1 &= k_1 S E_1 - (k_{-1} + k_2) C_1 \\
\dot{C}_2 &= k_3 S E_2 - (k_{-3} + k_4) C_2 \\
\dot{E}_1 &= -k_1 S E_1 + (k_{-1} + k_2) C_1 \\
\dot{E}_2 &= -k_3 S E_2 + (k_{-3} + k_4) C_2 \\
\dot{P}_1 &= k_2 C_1 \\
\dot{P}_2 &= k_4 C_2
\end{aligned}$$

The parameters k_i and k_{-i} are the rate constants of the reactions: k_1 and k_{-1} for the first reversible reaction (k_1 for the forward reaction and k_{-1} for the backward reaction), k_2 for the formation step of the first product P_1, k_3 and k_{-3} for the second reversible reaction, and finally k_4 for the formation step of the second product P_2.

The total concentration of the enzymes E_1 and E_2, both in free and in bound form, is constant: and equal to, say E_1^0 and E_2^0 respectively:

$$E_1(t) + C_1(t) = E_1^0, \text{ and } E_2(t) + C_2(t) = E_2^0$$

and thus we can eliminate E_1 and E_2 from the equations to get:

$$
\begin{aligned}
\dot{S} &= -k_1 S(E_1^0 - C_1) - k_3 S(E_2^0 - C_2) + k_{-1} C_1 + k_{-3} C_2 \\
\dot{C_1} &= k_1 S(E_1^0 - C_1) - (k_{-1} + k_2) C_1 \\
\dot{C_2} &= k_3 S(E_2^0 - C_2) - (k_{-3} + k_4) C_2 \\
\dot{E_1} &= -k_1 S(E_1^0 - C_1) + (k_{-1} + k_2) C_1 \\
\dot{E_2} &= -k_3 S(E_2^0 - C_2) + (k_{-3} + k_4) C_2 \\
\dot{P_1} &= k_2 C_1 \\
\dot{P_2} &= k_4 C_2
\end{aligned}
$$

Quasi-steady state

We make the following quasi-steady state assumptions:

$$\dot{C_1} = 0 = \dot{C_2}.$$

In other words, the two complexes SE_1 and SE_2 are assumed to be in steady state. Setting the corresponding equations in the model above equal to zero, yields:

$$
\begin{aligned}
0 &= k_1 S(E_1^0 - C_1) - (k_{-1} + k_2) C_1 \\
0 &= k_3 S(E_2^0 - C_2) - (k_{-3} + k_4) C_2
\end{aligned}
$$

We can solve these to express C_1 and C_2 in terms of S:

$$
\begin{aligned}
C_1 &= \frac{E_1^0 S}{S + \frac{k_{-1}+k_2}{k_1}} \\
C_2 &= \frac{E_2^0 S}{S + \frac{k_{-3}+k_4}{k_3}}
\end{aligned}
$$

The rates of product formation of P_1 and P_2 are respectively $dP_1/dt = k_2 C_1$ and $dP_2/dt = k_4 C_2$, and they take the usual Michaelis-Menten form:

$$\frac{dP_1}{dt} = \frac{V_{m1} S}{S + K_{m1}} \tag{1}$$

$$\frac{dP_2}{dt} = \frac{V_{m2} S}{S + K_{m2}} \tag{2}$$

with

$$V_{m1} = k_2 E_1^0 \text{ and } K_{m1} = \frac{k_{-1} + k_2}{k_1} \tag{3}$$

$$V_{m2} = k_4 E_2^0 \text{ and } K_{m2} = \frac{k_{-3} + k_4}{k_3} \tag{4}$$

Remark: Suppose we would consider only one of the reactions to take place, so that there is no competition for the substrate:

$$S + E_1 \longleftrightarrow C_1 \longrightarrow P_1 + E_1$$

In this case, making a similar quasi-steady state assumption, it can be shown that the rate of formation of P_1 is still be given by the Michaelis-Menten form (1) with the same expressions (3) for the maximal formation rate V_{m1} and half-saturation constant K_{m1}. A similar conclusion holds for the rate of formation of P_2.

In other words, whether one assumes the competition model or the single enzyme model

(no competition), the rate of formation of both products in terms of the substrate *S*, remains the same. This implies that when determining the values of V_m and K_m of both products experimentally, it does not matter whether this is done for the natural organism (which satisfies the competition model), or for the cloned system (which satisfies the single enzyme model).

Supplementary References

1 Curson, A. R. J., Todd, J. D., Sullivan, M. J. & Johnston, A. W. B. Catabolism of dimethylsulphoniopropionate: microorganisms, enzymes and genes. *Nature Reviews Microbiology*, 1-11, doi:10.1038/nrmicro2653 (2011).

2 Schneider, K., Asao, M., Carter, M. S. & Alber, B. E. *Rhodobacter sphaeroides* uses a reductive route via propionyl coenzyme A to assimilate 3-hydroxypropionate. *Journal of Bacteriology* **194**, 225-232, doi:10.1128/JB.05959-11 (2012).

3 Todd, J. D., Curson, A. R. J., Sullivan, M. J., Kirkwood, M. & Johnston, A. W. B. The *Ruegeria pomeroyi acuI* gene has a role in DMSP catabolism and resembles *yhdH* of *E. coli* and other bacteria in conferring resistance to acrylate. *PloS One* **7**, e35947, doi:10.1371/journal.pone.0035947 (2012).

4 Reisch, C. R. *et al.* Metabolism of dimethylsulphoniopropionate by *Ruegeria pomeroyi* DSS-3. *Molecular Microbiology* **89**, 774-791, doi:10.1111/mmi.12314 (2013).

5 Grote, J. *et al.* Streamlining and core genome conservation among highly divergent members of the SAR11 clade. *mBio* **3**, doi:10.1128/mBio.00252-12 (2012).

6 Sharpton, T. J. *et al.* Sifting through genomes with iterative-sequence clustering produces a large, phylogenetically diverse protein-family resource. *BMC Bioinformatics* **13**, 264, doi:10.1186/1471-2105-13-264 (2012).

7 Carini, P., Steindler, L., Beszteri, S. & Giovannoni, S. J. Nutrient requirements for growth of the SAR11 isolate '*Candidatus* Pelagibacter ubique' HTCC1062 on a defined medium. *ISME J* **7**, 592-602, doi:doi:10.1038/ismej.2012.122 (2013).

8 Smith, D. P. *et al.* Transcriptional and translational regulatory responses to iron limitation in the globally distributed marine bacterium Candidatus pelagibacter ubique. *Plos One* **5**, e10487, doi:10.1371/journal.pone.0010487 (2010).

9 Kevin, L. V. *et al.* High-resolution SAR11 ecotype dynamics at the Bermuda Atlantic Time-series Study site by phylogenetic placement of pyrosequences. *The ISME Journal* **7**, 1322-1332, doi:10.1038/ismej.2013.32 (2013).

10 Kirkwood, M., Le Brun, N. E., Todd, J. D. & Johnston, A. W. B. The *dddP* gene of *Roseovarius nubinhibens* encodes a novel lyase that cleaves dimethylsulfoniopropionate into acrylate plus dimethyl sulfide. *Microbiology* **156**, 1900-1906, doi:10.1099/mic.0.038927-0 (2010).

11 Sowell, S. M. *et al.* Transport functions dominate the SAR11 metaproteome at low-nutrient extremes in the Sargasso Sea. *ISME J* **3**, 93-105, doi:10.1038/ismej.2008.83 (2009).

12 Kiene, R. P., Williams, L. P. H. & Walker, J. E. Seawater microorganisms have a high affinity glycine betaine uptake system which also recognizes dimethylsulfoniopropionate *Aquatic Microbial Ecology* **15**, 39-51 (1998).

13 Rappé, M. S., Connon, S. A., Vergin, K. L. & Giovannoni, S. J. Cultivation of the

ubiquitous SAR11 marine bacterioplankton clade. *Nature* **418**, 630-633, doi:10.1038/nature00917 (2002).

14 Gibson, J. A. E., Garrick, R. C., Burton, H. R. & McTaggart, A. R. Dimethylsulfide and the algaPhaeocystis pouchetii in antarctic coastal waters. *Marine Biology* **104**, 339-346, doi:10.1007/bf01313276 (1990).

15 van Duyl, F. C., Gieskes, W. W. C., Kop, A. J. & Lewis, W. E. Biological control of short-term variations in the concentration of DMSP and DMS during a Phaeocystis spring bloom. *Journal of Sea Research* **40**, 221-231, doi:http://dx.doi.org/10.1016/S1385-1101(98)00024-0 (1998).

16 Zindler, C., Peeken, I., Marandino, C. A. & Bange, H. W. Environmental control on the variability of DMS and DMSP in the Mauritanian upwelling region. *Biogeosciences* **9**, 1041-1051, doi:10.5194/bg-9-1041-2012 (2012).

17 Varaljay, V. A. *et al.* Single-taxon field measurements of bacterial gene regulation controlling DMSP fate. *ISME J* **9**, 1677-1686, doi:10.1038/ismej.2015.23 (2015).

18 Kiene, R. in *Biological and Environmental Chemistry of DMSP and Related Sulfonium Compounds* (eds RonaldP Kiene, PieterT Visscher, MaureenD Keller, & GunterO Kirst) Ch. 29, 337-349 (Springer US, 1996).

19 Kiene, R. P. & Linn, L. J. Distribution and turnover of dissolved DMSP and its relationship with bacterial production and dimethylsulfide in the Gulf of Mexico. *Limnology and Oceanography* **45**, 849-861, doi:10.4319/lo.2000.45.4.0849 (2000).

20 Turner, S. M., Malin, G., Liss, P. S., Harbour, D. S. & Holligan, P. M. The seasonal variation of dimethyl sulfide and dimethylsulfoniopropionate concentrations in nearshore waters1. *Limnology and Oceanography* **33**, 364-375, doi:10.4319/lo.1988.33.3.0364 (1988).

21 Belviso, S. *et al.* Production of dimethylsulfonium propionate (DMSP) and dimethylsulfide (DMS) by a microbial food web. *Limnology and Oceanography* **35**, 1810-1821, doi:10.4319/lo.1990.35.8.1810 (1990).

22 Ledyard, K. M. & Dacey, J. W. H. Microbial cycling of DMSP and DMS in coastalandoligotrophicseawater. *Limnology and Oceanography* **41**, 33-40, doi:10.4319/lo.1996.41.1.0033 (1996).

23 Iverson, R. L., Nearhoof, F. L. & Andreae, M. O. Production of dimethylsulfonium propionate and dimethylsulfide by phytoplankton in estuarine and coastal waters. *Limnology and Oceanography* **34**, 53-67, doi:10.4319/lo.1989.34.1.0053 (1989).

24 Simó, R., Grimalt, J. O. & Albaigés, J. Dissolved dimethylsulphide, dimethylsulphoniopropionate and dimethylsulphoxide in western Mediterranean waters. *Deep Sea Research Part II: Topical Studies in Oceanography* **44**, 929-950, doi:http://dx.doi.org/10.1016/S0967-0645(96)00099-9 (1997).

25 Simó, R., Pedrós-Alió, C., Malin, G. & Grimalt, J. O. Biological turnover of DMS, DMSP and DMSO in contrasting open-sea waters. *Marine Ecology Progress Series* **203**, 1-11, doi:10.3354/meps203001 (2000).

26 Kiene, R. P. & Slezak, D. Low dissolved DMSP concentrations in seawater revealed by small-volume gravity filtration and dialysis sampling. *Limnology and Oceanography: Methods* **4**, 80-95, doi:10.4319/lom.2006.4.80 (2006).

27 Bradford, M. M. A rapid and sensitive method for the quantitation of microgram

quantities of protein utilizing the principle of protein-dye binding. *Anal Biochem* **72**, 248-254, doi:S0003269776699996 [pii] (1976).

28 Todd, J. D. *et al.* Molecular dissection of bacterial acrylate catabolism--unexpected links with dimethylsulfoniopropionate catabolism and dimethyl sulfide production. *Environmental microbiology* **12**, 327-343, doi:10.1111/j.1462-2920.2009.02071.x (2010).

29 Eddy, S. R. What is a hidden Markov model? *Nature Biotechnology* **22**, 1315-1316 (2004).

30 Eddy, S. R. Profile hidden Markov models. *Bioinformatics* **14**, 755 (1998).

31 Boden, R. *et al.* Purification and characterization of dimethylsulfide monooxygenase from *Hyphomicrobium sulfonivorans*. *Journal of Bacteriology* **193**, 1250-1258, doi:10.1128/JB.00977-10 (2011).

32 McDevitt, C. A., Hugenholtz, P., Hanson, G. R. & McEwan, A. G. Molecular analysis of dimethyl sulphide dehydrogenase from *Rhodovulum sulfidophilum*: its place in the dimethyl sulphoxide reductase family of microbial molybdopterin - containing enzymes. *Molecular Microbiology* **44**, 1575-1587 (2002).

33 Reisch, C. R., Moran, M. A. & Whitman, W. B. Bacterial catabolism of dimethylsulfoniopropionate (DMSP). *Frontiers in Microbiology* **2**, 172, doi:10.3389/fmicb.2011.00172 (2011).

34 Eddy, S. R. Accelerated profile HMM searches. *PLoS Computational Biology* **7**, e1002195 (2011).

35 Wilhelm, L. J., Tripp, H. J., Givan, S. A., Smith, D. P. & Giovannoni, S. J. Natural variation in SAR11 marine bacterioplankton genomes inferred from metagenomic data. *Biology Direct* **2**, 27, doi:10.1186/1745-6150-2-27 (2007).

36 Monroe, M. E., Shaw, J. L., Daly, D. S., Adkins, J. N. & Smith, R. D. MASIC: a software program for fast quantitation and flexible visualization of chromatographic profiles from detected LC-MS(/MS) features. *Computational Biology Chemistry* **32**, 215-217, doi:10.1016/j.compbiolchem.2008.02.006 (2008).

37 Keller, A. & Shteynberg, D. Software pipeline and data analysis for MS/MS proteomics: the trans-proteomic pipeline. *Methods in Molecular Biology* **694**, 169-189, doi:10.1007/978-1-60761-977-2_12 (2011).

38 Vizcaino, J. A. *et al.* ProteomeXchange provides globally coordinated proteomics data submission and dissemination. *Nature Biotechnology* **32**, 223-226, doi:10.1038/nbt.2839 (2014).